Redox Biology 29 (2020) 101376

Contents lists available at ScienceDirect

Redox Biology

journal homepage: www.elsevier.com/locate/redox

A FABP4-PPARγ signaling axis regulates human monocyte responses to electrophilic fatty acid nitroalkenes

M. Lamas Bervejillo[a], J. Bonanata[b,c], G.R. Franchini[d], A. Richeri[e], J.M. Marqués[f], B.A. Freeman[g], F.J. Schopfer[g], E.L. Coitiño[b,c,**], B. Córsico[d], H. Rubbo[c,h], A.M. Ferreira[a,*]

[a] Laboratorio de Inmunología, Instituto de Higiene, Facultad de Ciencias/Facultad de Química, Universidad de la República (UdelaR), Montevideo, CP 11600, Uruguay
[b] Laboratorio de Química Teórica y Computacional, Instituto de Química Biológica, Facultad de Ciencias, UdelaR, Montevideo, CP 11400, Uruguay
[c] Centro de Investigaciones Biomédicas (CeInBio), UdelaR, Montevideo, CP 11800, Uruguay
[d] Instituto de Investigaciones Bioquímicas de La Plata (INIBIOLP), Facultad de Ciencias Médicas, Universidad Nacional de La Plata, La Plata, Argentina
[e] Laboratorio de Biología Celular, Departamento de Neurofarmacología Experimental, Instituto de Investigaciones Biológicas Clemente Estable, Montevideo, CP 11600, Uruguay
[f] Laboratorio de Investigación en Vacunas, Departamento de Desarrollo Biotecnológico, Instituto de Higiene, Facultad de Medicina, UdelaR, Montevideo, CP 11600, Uruguay
[g] Department of Pharmacology and Chemical Biology, University of Pittsburgh, Pittsburgh, PA, 15213, USA
[h] Departamento de Bioquímica, Facultad de Medicina, UdelaR, Montevideo, CP 11800, Uruguay

ARTICLE INFO

Keywords:
Nitro-fatty acids
Peroxisome proliferator-activated receptor gamma
Fatty acid binding protein 4
Monocytes
Macrophages
Lipid signaling

ABSTRACT

Nitro-fatty acids (NO_2-FA) are electrophilic lipid mediators derived from unsaturated fatty acid nitration. These species are produced endogenously by metabolic and inflammatory reactions and mediate anti-oxidative and anti-inflammatory responses. NO_2-FA have been postulated as partial agonists of the Peroxisome Proliferator-Activated Receptor gamma (PPARγ), which is predominantly expressed in adipocytes and myeloid cells. Herein, we explored molecular and cellular events associated with PPARγ activation by NO_2-FA in monocytes and macrophages. NO_2-FA induced the expression of two PPARγ reporter genes, Fatty Acid Binding Protein 4 (*FABP4*) and the scavenger receptor *CD36*, at early stages of monocyte differentiation into macrophages. These responses were inhibited by the specific PPARγ inhibitor GW9662. Attenuated NO_2-FA effects on PPARγ signaling were observed once cells were differentiated into macrophages, with a significant but lower *FABP4* up-regulation, and no induction of *CD36*. Using *in vitro* and *in silico* approaches, we demonstrated that NO_2-FA bind to FABP4. Furthermore, the inhibition of monocyte FA binding by FABP4 diminished NO_2-FA-induced upregulation of reporter genes that are transcriptionally regulated by PPARγ, Keap1/Nrf2 and HSF1, indicating that FABP4 inhibition mitigates NO_2-FA signaling actions. Overall, our results affirm that NO_2-FA activate PPARγ in monocytes and upregulate FABP4 expression, thus promoting a positive amplification loop for the downstream signaling actions of this mediator.

1. Introduction

Nitrated derivatives of unsaturated fatty acids (NO_2-FA) mediate pleiotropic cell signaling actions [1,2]. NO_2-FA are endogenously generated upon nitrogen dioxide ($\cdot NO_2$) addition to double bonds [3]. Among unsaturated fatty acids, those containing conjugated diene moieties are preferential substrates for nitration, because of the greater reactivity of the external flanking carbons of the conjugated diene moiety [4]. Conjugated linoleic acid (CLA), the most abundant dietary conjugated fatty acid, has been identified as a major endogenous substrate for nitration, generating nitro conjugated linoleic acid (NO_2-CLA) [5]. In healthy humans, CLA nitration occurs during digestion of lipid-containing foods, leading to nanomolar concentrations of unesterified NO_2-CLA in plasma [6]. Current data indicate that NO_2-CLA levels rise in metabolically-stressed and/or inflamed tissues because of downstream nitro-oxidative reactions stemming from nitric oxide synthase

* Corresponding author. Laboratorio de Inmunología, Instituto de Higiene, Facultad de Ciencias/Facultad de Química, Universidad de la República (UdelaR), Montevideo, CP 11600, Uruguay.
** Corresponding author. Laboratorio de Química Teórica y Computacional, Instituto de Química Biológica, Facultad de Ciencias, UdelaR, Montevideo, CP 11400, Uruguay.
E-mail addresses: laurac@fcien.edu.uy (E.L. Coitiño), aferrei@fq.edu.uy (A.M. Ferreira).

https://doi.org/10.1016/j.redox.2019.101376
Received 2 August 2019; Received in revised form 14 October 2019; Accepted 6 November 2019
Available online 10 November 2019

induction in inflammatory cells and tissues [2,7,8]. Despite the much lower reactivity of monounsaturated fatty acids, low levels of nitrated oleic acid have been reported in human plasma [9].

NO_2-FA modulate cell metabolic and inflammatory responses [5,10–17] by multiple mechanisms, predominantly those involving post-translational modifications (PTM) of target proteins that regulate intracellular signaling responses and gene expression. These PTMs are a consequence of the soft electrophilic nature of NO_2-FA, which promotes reversible Michael addition reactions with soft nucleophilic groups such as His or Cys in proteins, leading to alterations in protein cell distribution and/or function [18]. The nuclear receptor PPARγ (*Peroxisome Proliferator-Activated Receptor γ*) is one target of NO_2-FA. PPARγ is a multi-domain protein with high affinity for lipophilic ligands. Agonists stabilize the active state of PPARγ, regulating the expression of genes involved in lipid metabolism or inflammation [19,20]. NO_2-FA bind to the PPARγ ligand-binding domain (LBD) and covalently react with a redox-sensitive Cys-285 in the LBD, partially activating the transcriptional function of the receptor [21–25]. This contrasts with the PPARγ activation profile induced by stronger ligands or full agonists such as the family of synthetic thiazolidinedione activators [26]. Besides PPARγ, Keap1 (*Kelch-like ECH-associated protein 1*) was described as a NO_2-FA target with implications for cytoprotective responses [27–30]. NO_2-FA react with key cysteine residues in Keap1, resulting in reduced proteasomal degradation of the transcription factor Nrf2 (*Nuclear factor-erythroid 2-related factor 2*), and activation of Nrf2-dependent transcription of anti-oxidant and detoxifying genes, such as heme oxygenase-1 (*HMOX1*) and glutamate cysteine ligase modulatory gene (*GCLM*). Finally, NO_2-FA adduction to members of the heat shock protein family (HSP) that sense electrophiles, leads to activation of HSF1-regulated gene expression [30] and downstream anti-inflammatory effects in myeloid cells [31,32]. This NO_2-FA signaling mechanism in endothelial cells stimulates *HSPA1A* expression [28]. Beyond the pleiotropic nature of NO_2-FA, their protein targets will depend on several factors including cell redox and activation status as well as the intracellular half-life and stability of NO_2-FA.

The effect of NO_2-FA on PPARγ activation has primarily been studied in a metabolic context using fibroblasts, adipocytes, mammary epithelial (MCF7), or kidney cell lines (CV-1) [33–35]. Reporter assays have also been used but do not reliably reproduce physiological PPARγ expression levels and interactions with co-regulators (co-activators and co-repressors) that modulate its transcriptional activity [21–23]. In aggregate, NO_2-FA activation of PPARγ and subsequent modulation of cell functions is still poorly understood, particularly in the context of immunological responses. Monocytes and macrophages are innate cell populations of foremost importance in mediating integrated inflammatory responses, eliminating pathogens and contributing to tissue homeostasis. The recruitment of monocytes and their subsequent differentiation into macrophages gains relevance during inflammation to reinforce the immune response. Previously, PPARγ-independent effects on monocyte and macrophage inflammatory responses to NO_2-FA have been reported [10,36]. In this work, we examined NO_2-FA activation of PPARγ in both human monocytes undergoing differentiation into macrophages (termed differentiating monocytes) and macrophages.

We report herein that low μM levels of NO_2-FA activated PPARγ in differentiating monocytes and to a lesser extent in already-differentiated macrophages. The most robust PPARγ-regulated gene expression response in these cells was the upregulation of *FABP4*, a member of the fatty acid-binding protein family (FABP) that transports fatty acids between cell compartments [37]. NO_2-FA have limited solubility in aqueous milieu, thus this *FABP4* upregulation and transport capability induced a significant impact on NO_2-FA trafficking to nuclear and cytoplasmic targets including PPARγ, in turn regulating downstream cell signaling responses. These responses were abrogated by FABP4 inhibitors in differentiating monocytes, affirming that FABP4 plays a crucial role in the transduction of NO_2-FA by (at least) PPARγ, Keap1/Nrf2 and HSP-regulated signaling networks.

2. Materials and methods

2.1. Chemical reagents

Reagents of analytical grade were purchased from Sigma (St. Louis, MO, USA) unless otherwise stated. Octadec-9-enoic acid (oleic acid, OA), octadec-9,11-dienoic acid (conjugated linoleic acid, CLA) and 5,8,11,14-eicosatetraenoic acid (arachidonic acid, AA) were obtained from Nu-Check Prep, Inc (Elysian, MN, USA). 9- and 12-nitro-octadec-9,11-dienoic acid (9-NO_2-CLA and 12-NO_2-CLA), 9- and 10-nitro-octadec-9-enoic acid (9-NO_2-OA and 10-NO_2-OA) and 10-nitro-octadecanoic acid (NO_2-SA) were synthesized as described previously [5,38,39]. The terms NO_2-CLA and nitro oleic acid (NO_2-OA) refer to the mixture of the corresponding above-mentioned positional isomers. AA nitration was carried out as previously described [11] to obtain a mixture of positional isomers referred to as nitroarachidonic acid (NO_2-AA). Rosiglitazone (Rosi), GW9662, and HTS01037 (HTS) were obtained from Cayman Chem (USA) while BMS 309403 (BMS) was acquired from ApexBio (USA).

2.2. Recombinant mouse FABP4 and rabbit anti-mouse FABP4 polyclonal antibodies

Recombinant mouse FABP4 (rFABP4) was expressed and purified following conventional protocols as previously described (Supplementary Fig. 1) [40]. Polyclonal antiserum against rFABP4 was raised in rabbits following standard protocols. All procedures were carried out in accordance with the ethical guidelines of the Honorary Commission of Animal Experimentation (CHEA) from UdelaR. Briefly, a New Zealand rabbit was injected subcutaneously with 500 μg of purified rFABP4 in an emulsion made of water in oil, prepared with Incomplete Freund Adjuvant. A second dose (booster) was similarly performed when the serum antibody titer anti-rFABP4 significantly dropped (about 16-times lower than the maximum reached). Bleeding was done at day 47 post-booster. The polyclonal antisera obtained showed a titer of 1/48.000 by ELISA and showed to recognize by Western blot a 14 kDa band present in a THP-1 cell extract, which was compatible with FABP4. The fraction of polyclonal anti-rFABP4 antibodies was purified by immunoaffinity using rFABP4 conjugated to NHS-Sepharose and 0.1 M glycine pH 2.0 for elution. In parallel, we obtained the polyclonal antisera fraction non-specifically bound to Sepharose as a control.

2.3. Cell culture for NO_2-FA stimulation

Human pre-monocytic THP-1 cells (ATCC, USA), a suitable model of primary human monocytes and macrophages [41], was used. Cells were cultured in RPMI medium (RPMI 1640 supplemented with 10 mM HEPES, 1.5 g/L sodium bicarbonate, 1 mM sodium pyruvate, 2 mM glutamine, 100 U/mL penicillin, 0.1 mg/mL streptomycin and 250 ng/mL amphotericin B) plus 10% fetal bovine serum (FBS, GIBCO). Cells were maintained at 37 °C in a humidified atmosphere of 5% CO_2 in air, and subcultured every 3–4 days to maintain cell density between 0.2 and 1.0 × 10^6 cells/mL. Cells were plated at 5 × 10^5 cells/well in RPMI medium supplemented with 5% FBS and macrophage differentiation was induced with 50 ng/mL phorbol esters (PMA, SIGMA). NO_2-FA, their corresponding fatty acid precursors (FA) and Rosi (a well-known PPARγ ligand) were tested at a final concentration of 1 μM, and the vehicle (DMSO) was used as a negative control. For assessing effects on differentiating monocytes, tested compounds were added together with PMA. For assessing effects on completely differentiated macrophages, macrophages were obtained after 72 h differentiation with PMA, cultured in RPMI medium without PMA for 48 h, and subsequently stimulated with NO_2-FA, Rosi or controls. In all assays, stimulation was stopped after 6 h or 16 h stimulation for mRNA levels and protein synthesis analysis, respectively. In order to evaluate the contribution of

PPARγ activation to NO_2-FA-induced effects, similar experiments were done in the presence of a PPARγ inhibitor, GW9662. Briefly, cells were treated with PMA for 3.5 h, and then for 30 min with GW9662 (1 or 2.5 μM). Cells were then stimulated with NO_2-FA or controls and mRNA and protein levels examined at 6 h or 16 h post-stimulation, respectively. The role of FABP4 on NO_2-FA cell signaling actions was evaluated using the FABP4 inhibitors BMS [42] and HTS [43] in the presence of 5% delipidated FBS (PAN Biotech, Germany). Cells were pretreated with PMA together with BMS (25 μM) or HTS (15 μM) for 2 h and then stimulated with NO_2-FA or controls for 6 h mRNA expression was then examined as described below. In the case of HTS, an additional pre-incubation (24 h) was carried as previously described [44].

2.4. Cell viability

Cell viability was analyzed using the MTT [3-(4,5-dimethylthiazol-2-yl)-2,5-diphenyl-2H-tetrazolium bromide] assay. Briefly, cells were cultured in the presence 200 μg/ml of MTT in PBS with 0.1% glucose for 3 h at 37 °C, 5% CO_2. Afterward, cells were washed with PBS, formazan was dissolved in DMSO and the absorbance at 560 nm was measured. In the case of differentiating monocytes, it was also analyzed on the basis of exclusion of the fixable viability dye (LIVE/DEAD, Invitrogen) and measured by flow cytometry.

2.5. Gene expression analysis

After stimulation, total cellular mRNA was isolated from cells using the TRIzol Reagent (Ambion, Life Technologies, USA) accordingly to the manufacturer's recommendations. Traces of DNA were removed by treatment with DNAse-I following the manufacturer's instructions (Fermentas, Thermo Fisher Scientific, USA). The synthesis of the first strand complementary DNA (cDNA) was carried out using 1 μg of total mRNA, M-MLV reverse transcriptase (200 Units, Life Technologies, USA), 0,5 mM dNTPs, 5 μM random primers, Ribolock (40 Units, Fermentas) at 25 °C for 10 min, followed by 37 °C for 50 min and 70 °C for 15 min. Template DNA was amplified by quantitative real-time PCR using Quantitect SYBR Green PCR kit (Qiagen, Hilden-Germany) in a Rotor-Gene Q real-time PCR cycler (Qiagen), according to the following protocol: 15 min at 95 °C, followed by 40 cycles at 94 °C for 15 s, at 50 °C for 30 s and at 72 °C for 30 s.

The primers, designed using Primer Express software (Applied Biosystems, USA), are listed in Table 1 and were used at a final concentration of 0.9 μM. The expression of genes of interest was normalized using *GAPDH* as housekeeping gene, except for assays using BMS where *18S* was used. The relative mRNA amount in each sample was estimated using the $2^{-\Delta\Delta Ct}$ method [45], where ΔCt = Ct gene of interest-Ct housekeeping, and expressed as relative mRNA levels in the test group compared to the control group.

2.6. FABP4 detection by immunofluorescence

THP-1 cells (5×10^5 cells) were seeded on coverslips and stimulated with PMA (50 ng/mL) plus 1 μM concentration of NO_2-FA, FA, Rosi or DMSO (vehicle) in RPMI supplemented with 5% fetal delipidated FBS, for 10 h at 37 °C and in a humidified atmosphere of 5% CO_2. Cells were subsequently fixed with 4% paraformaldehyde in PBS, and coverslips were incubated overnight at 4 °C with the affinity-purified rabbit anti-rFABP4 antibody (1:100) or the corresponding control antibody. After washing 3 times with PBS, cells were stained using goat anti-rabbit IgG (H + L) conjugated with Alexa Fluor TM 488 (1:1600, Invitrogen) for 1.5 h, and then with DAPI (300 μM, Calbiochem-Novabiochem, USA) for 30 min. Cells were observed under epifluorescence microscopy (Nikon E800, Japan). To measure FABP4 nuclear translocation, cells were similarly stimulated for 10 h with PMA plus 1 μM NO_2-FA in order to reach detectable FABP4 levels, Leptomycin B (10 ng/ml) was added for 30 min and a short re-stimulation (30 or 60 min) with NO_2-FA, FA or Rosi (between 1 and 10 μM) was performed. Cells were stained as described above, but also using DAPI and rhodamine-phalloidin (0.3 μg/ml, Santa Cruz Biotechnology, USA) for nuclear and actin staining, respectively. Images were obtained with an LSM 800-AiryScan confocal microscope (Zeiss, Germany) and processed using FIJI/ImageJ [46]. Quantification was performed using at least 30 cells per condition in three independent experiments. The nucleus and the whole cell were delimitated according to DAPI and rhodamine staining, respectively, and integrated density (selected area*mean grey value, ID) was measured for each cell compartment. FABP4 distribution was analyzed by determining the nuclear/cytoplasm ratio, calculated as the Nuclear ID/(Total ID – Nuclear ID) (N/T-N).

2.7. FABP4 detection in cell extracts by Western blot

THP-1 cell extracts were obtained after 16 h of NO_2-FA stimulation. Briefly, monocytes were washed two times with RPMI without FBS at 37 °C, lysed using hypotonic buffer (Hepes 10 mM, EDTA 0.5 mM, KCl 10 mM, DTT 1 mM and protease inhibitor cocktail SIGMA, pH 7.5) and sonicated (three rounds of 1 min pulses at 15% and 30% of total potency) using an Omni-Ruptor 4000 (OMNI International Inc.). Samples were analyzed by SDS-PAGE at reducing conditions using polyacrylamide 12.5% gels and following conventional protocols. The proteins were transferred to a PVDF membrane (Millipore) and, after blocking with PBS 0.5% bovine serum albumin (BSA), probed with rabbit anti-rFABP4 antisera (1:20000 in PBS containing 0.05% BSA and 0.05% Tween 20) or rabbit anti-human tubulin IgG (1:1000, Cell Signaling, USA) followed by peroxidase-conjugated anti-rabbit IgG (1:2000, Calbiochem). Detection was carried out using SuperSignal West Pico Chemiluminescent Substrate (Thermo Fischer Scientific) in an imaging system (G:BOX, Syngene, India).

Table 1
Primers for real-time PCR.

Gene	Forward primer	Reverse primer
18S	GTAACCCGTTGAACCCCATT	CCATCCAATCGGTAGTAGCG
ABCA-1	TTTCCAGGCCAGTACGGAAT	TCGCCAAACCAGTAGGACTT
ABCG-1	CTGACATTTCCCCTGGAGATG	TCCAGTACACGATGCTGCAGTA
CD36	GTGGCAGCTGCATCCCATAT	TCTGACTTGGAACATAGAAGATTTTGA
CPT1A	GGTGGTGGGCGTGATGA	CAGTTGGCCGTTTCCAGAGT
FABP4	GCCAGGAATTTGACGAAGTCAC	TTCTGCACATGTACCAGGACAC
FABP5	CCCTGGGAGAGAAGTTTGAAGA	AATGCACCATCTGTAAAGTTGCA
GAPDH	ACCCACTCCTCCACCTTTG	CTCTTGTGCTCTTGCTGGG
GCLM	AGACGGGGAACCTGCTGAA	TCATGAAGCTCCTCGCTGTC
HO1	AAGACTGCGTTCCTGCTCAA	GGGGGCAGAATCTTGCACTT
HSP70	CCACCAAGCAGACGCAGAT	GCCCTCGTACACCTGGATCA
Il1B	TTGGTGATGTCTGGTCCATATGA	GGACATGGAGAACACCACTTGTT
MCP1	GCTCAGCCAGATGCAATCAA	GCCTCTGCACTGAGATCTTCCT
PPARG	CAACAGACAAATCACCATTCGTTAT	GGATGGCCACCTCTTTGCT

2.8. CD36 detection by flow cytometry

Stimulated THP-1 monocytes (1×10^6 cells/well) were washed twice with cold PBS and detached by treatment with PBS containing 1 mM EDTA, 0.1% NaN_3, 0.1% glucose (PBS_{FC} buffer) for 10 min at 4 °C. After blocking with PBS_{FC} supplemented with 0.1% SFB, cells were incubated with mouse IgM anti-human CD36 (BD Biosciences, USA) or with an IgM isotype control (BD Biosciences) following manufacturer's recommendations. Then, cells were washed 3 times and development was carried out by incubation with phycoerythrin-conjugated anti-mouse IgM (BD Biosciences) according to the manufacturer's protocol. Cells were recorded on a FACSCalibur equipment (BD Biosciences) and analyzed with FlowJo (version 7.6, USA, www.flowjo.com).

2.9. FABP4 binding assays

The fluorimetric binding assay was performed as previously described [47]. rFABP4 (3 μM) was incubated with the hydrophobic fluorescence probe 8-anilinonaphthalene-1-sulfonic acid (ANS, 10 μM, Molecular Probes) for 5 min in 1 mL final volume of phosphate buffer (5 mM K_2HPO_4, 5 mM KH_2PO_4, 150 mM KCl, pH 7,4). Using a Fluorolog-3 (Horiba-Yvon) spectrofluorometer, the probe was excited at 400 nm (excitation slit 1), and emission spectra was registered between 420 and 600 nm (emission slit 2) at 25 °C, using FluorEssence™ software. Then, small amounts of the NO_2-FA were added progressively and the emission spectrum was registered 2 min after each addition to reach FABP4 saturation. NO_2-CLA, NO_2-OA, and NO_2-AA were tested and compared with their FA precursors (CLA, OA and AA, respectively). Each experiment was done at least in triplicates. Fluorescence data were fitted to a hyperbolic decay using SigmaPlot (version 11.0, Systat Software, Inc., USA, www.systatsoftware.com). The apparent dissociation constant (K_{dapp}) was calculated using the equation $EC_{50ligand}/[ANS] = K_{d,ligand}/K_{d,ANS}$ as previously described [48]. To obtain $K_{d,ANS}$, FABP4 (2 μM) was titrated with the fluorescent probe until reaching saturation. Curves were fitted using SigmaPlot to a one-site ligand binding saturation model, and $K_{d,ANS}$ was calculated as the mean of four independent experiments.

2.10. In silico prediction and analysis of FA and NO_2-FA binding to murine FABP4 in 1:1 complexes

The crystallographic structure of the available murine mFABP4:oleate complex in the open portal (inactive for translocation) conformation (PDB 1LID) [49] was taken as starting point for constructing the corresponding mFABP4:FA or mFABP4:NO_2-FA 1:1 complexes in solution and running 1.2 μs molecular dynamics (MD) NPT simulations at 310 K and 1 atm using the AMBER 16 suite [50] (see details on the simulations and trajectory analysis in the supplementary information). The study included OA and conjugated CLA, and the corresponding regioisomeric nitroalkene derivatives (9-/10-NO_2-OA and 9-/12-NO_2-CLA) as ligands, whose anionic structure in solution was determined by Density Functional Theory (DFT) quantum mechanics (QM) calculations [51] in a IEF-PCM continuous solvent [52] using Gaussian09 [53] (details on QM modeling in the supplementary information). Representative structures for each of the six complexes under study were obtained from MD by hierarchical-agglomerative clustering analysis and the presence of active/inactive for translocation conformations was monitored inspecting the distance between Phe57 (*βC-βD* loop) and Thr29 (*αII* helix) along the trajectories with *cpptraj,* taking values smaller than 8.5 Å as indicative of a closed conformation. In order to analyze the trends on binding affinity along the series of FA/NO_2-FA looking for evidence on eventual regioisomeric modulation, MM/PB(GB)SA binding free energies [54] were also obtained within a single-trajectory approach, extracting 201 snapshots from the 1.2 μs MD simulations separated every 500 ns (the first 200 ns were discarded) with the *mmpbsa.py* module [55] of AmberTools17 [50].

2.11. Data analysis

All experiments were performed at least three independent times (n = 3) in duplicate. Statistical analysis was carried out with GraphPad Prism (version 5, GraphPad Software, USA, www.graphpad.com) using two-way analysis of variance (ANOVA) for multiple comparisons, with Tukey post-test, or one-way ANOVA with Dunn post-test as indicated. For immunofluorescence studies, when comparing two groups, an unpaired *t*-test was used. Differences were considered significant when $p \leq 0.05$.

3. Results

3.1. NO_2-FA activate PPARγ in differentiating monocytes and to a lesser extent in macrophages

For studying the ability of NO_2-FA to activate PPARγ in differentiating monocytes and macrophages, cell response to the full PPARγ agonist Rosiglitazone (Rosi) was firstly examined by quantitative analysis of mRNA expression of a series of potential PPARγ reporter genes (Supplementary Fig. 2). *FABP4* was the most upregulated gene in both cell types, exhibiting the highest increment at 6 h post-stimulation (about 20-fold and 3-fold, Supplementary Figs. 2e and 2f, respectively). *FABP5* and *CD36* expression were moderately upregulated by Rosi in differentiating monocytes and macrophages, with increases slightly higher in monocytes than macrophages. Regarding *ABCA1, ABCG1,* and *CPT1A*, Rosi induced dissimilar and modest responses in monocytes and macrophages. Based on these results, *FABP4*, *FABP5,* and *CD36* were chosen as target genes for studying the effect of NO_2-FA on PPARγ activation.

Studies were carried out using low micromolar concentrations of NO_2-OA, NO_2-CLA, and NO_2-AA (up to 1 μM), which are likely close to physiological levels in an inflammatory milieu [17] and did not cause alterations in cell viability (Supplementary Fig. 3). We found that all NO_2-FA, but not their corresponding FA precursors, were able to induce statistically significant increases in FABP4 mRNA levels in differentiating monocytes (Fig. 1a), showing the relevance of nitration for PPARγ activation. In contrast, FABP5 mRNA levels were unchanged after NO_2-FA stimulation (Fig. 1b) and only NO_2-CLA caused a modest increment in CD36 mRNA levels, suggesting that NO_2-CLA was the most potent PPARγ activator among tested NO_2-FA (Fig. 1c). In macrophages, NO_2-FA stimulation led to increases in FABP4 mRNA levels (Fig. 1e), but the magnitude of these increases was much lower than that observed in monocytes (1.6-fold vs. 7.5-fold for NO_2-CLA, respectively). Furthermore, no changes in *FABP5* and *CD36* expression were observed in macrophages after NO_2-FA stimulation while, as expected, Rosi induced significant rises in these PPARγ target genes (Fig. 1f and g). Moreover, we measured *PPARG* mRNA levels in both cell types to determine whether Rosi and NO_2-FA effects could induce an increase in *PPARG* expression. Results showed that exposure to Rosi and NO_2-FA did not significantly affect *PPARG* expression (Fig. 1d and h). In aggregate, these results indicate that NO_2-FA could act as partial PPARγ agonists in human differentiating monocytes and, to a lesser extent, in human macrophages, enhancing the transcription of genes associated with lipid metabolism such as *CD36* and *FABP4*.

Next, we analyzed whether upregulation of *FABP4* and *CD36* transcription by NO_2-FA-stimulation led to an increment in protein levels. To that end, FABP4 levels were determined by immunofluorescence, using affinity-purified anti-rFABP4 antibodies or its corresponding control. In agreement with the effects observed at the mRNA level, stimulation of differentiating monocytes with Rosi or NO_2-FA, but not with native FA, led to significant increases in FABP4 protein expression (Fig. 2a and b). No reactivity was observed using control antibodies (Supplementary Fig. 4). FABP5 might cause cross-reactivity in this assay because of its similar amino acid sequence and 3D-structure to FABP4 (Supplementary Fig. 5). However, the fluorescence response was

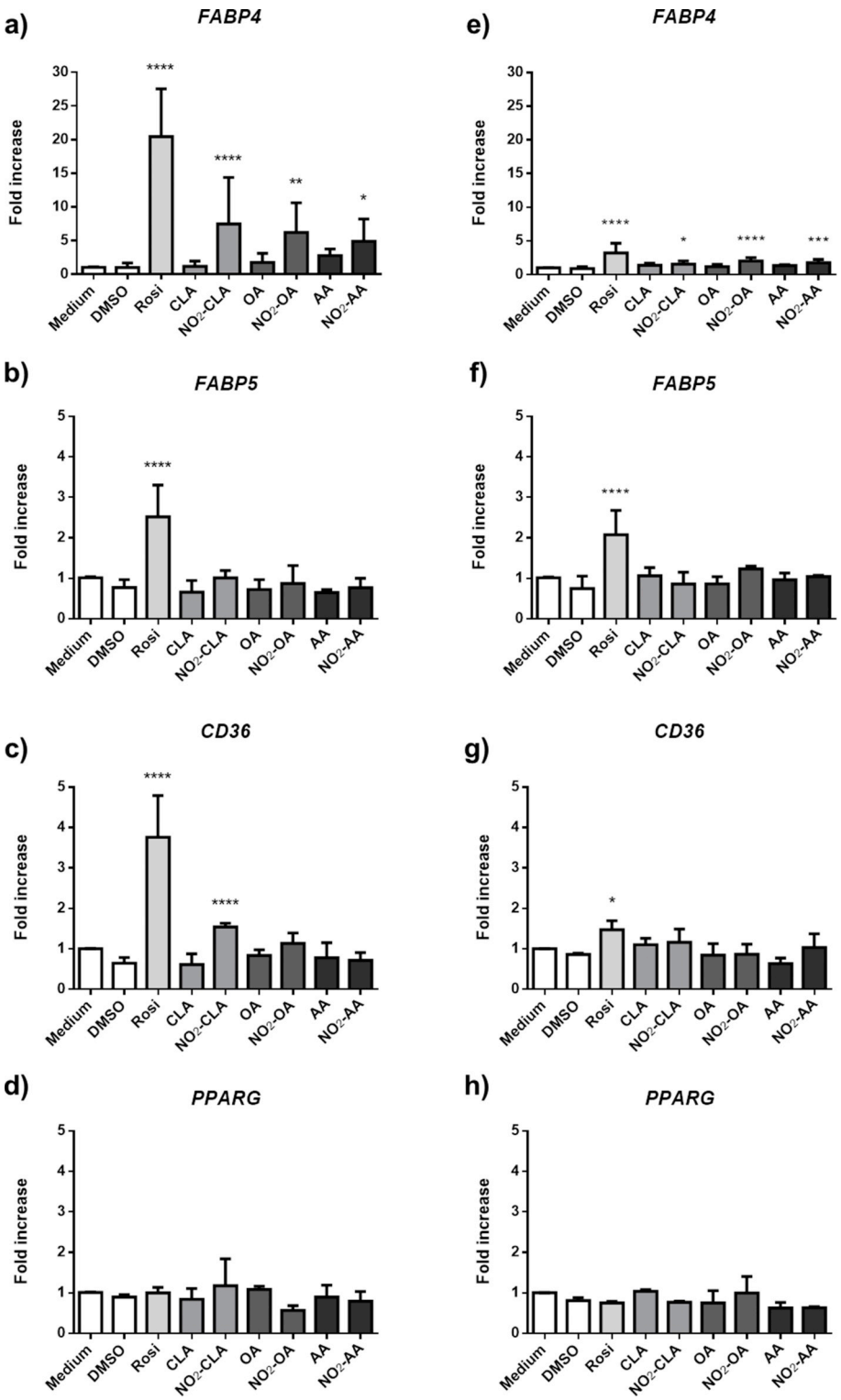

Fig. 1. NO_2-FA stimulated **FABP4 and CD36 mRNA** expression **in differentiating monocytes, and to a lesser extent in macrophages**.
Differentiating THP-1 monocytes **(a, b, c, d)** and THP-1 macrophages **(e, f, g, h)**, obtained by treatment with PMA, were stimulated with 1 μM concentration of Rosi, NO_2-FA or their corresponding FA precursors. In parallel, cells were incubated with DMSO (vehicle) as a control. After 6 h stimulation, cells were homogenized to obtain total mRNA, and *FABP4*, *FABP5, CD36* and *PPARγ* mRNA levels were determined by real-time-qPCR and normalized to the housekeeping gene *GAPDH*. Results are represented as relative mRNA levels (fold increase) referred to Medium group, and correspond to the mean of at least three independent experiments ± SD. (*) Indicates statistically significant differences compared with DMSO (Two-way ANOVA, Tukey's Multiple Comparison test * $p^{<}0.05$, ** $p^{<}0.01$, *** $p^{<}0.001$, **** $p^{<}0.0001$).

due to upregulation of *FABP4* expression since FABP5 mRNA levels were unchanged after NO_2-FA stimulation of differentiating monocytes (Fig. 1b). A contrasting scenario was observed in macrophages, in which NO_2-FA treatment did not lead to increases in FABP4 protein levels (Fig. 2c). Moreover, Rosi was unable to increase FABP4 protein expression, despite an ability to enhance *FABP4* transcription (Fig. 1e), suggesting that FABP4 synthesis might have reached a plateau under these conditions. On the other hand, CD36 protein levels were determined by flow cytometry. Among the tested NO_2-FA, only NO_2-CLA caused a weak, but statistically significant rise in CD36 protein expression in differentiating monocytes (Fig. 2d), which correlates with its ability to upregulate *CD36* transcription.

Considering the robustness of NO_2-FA transcriptional responses and their impact on protein expression, studies were then focused on differentiating monocytes. The role of PPARγ on NO_2-FA induction of *FABP4* and *CD36* expression was evaluated using the PPARγ specific inhibitor GW9662. GW9662 treatment inhibited *FABP4* and *CD36* mRNA induction triggered by Rosi and NO_2-FA in differentiating

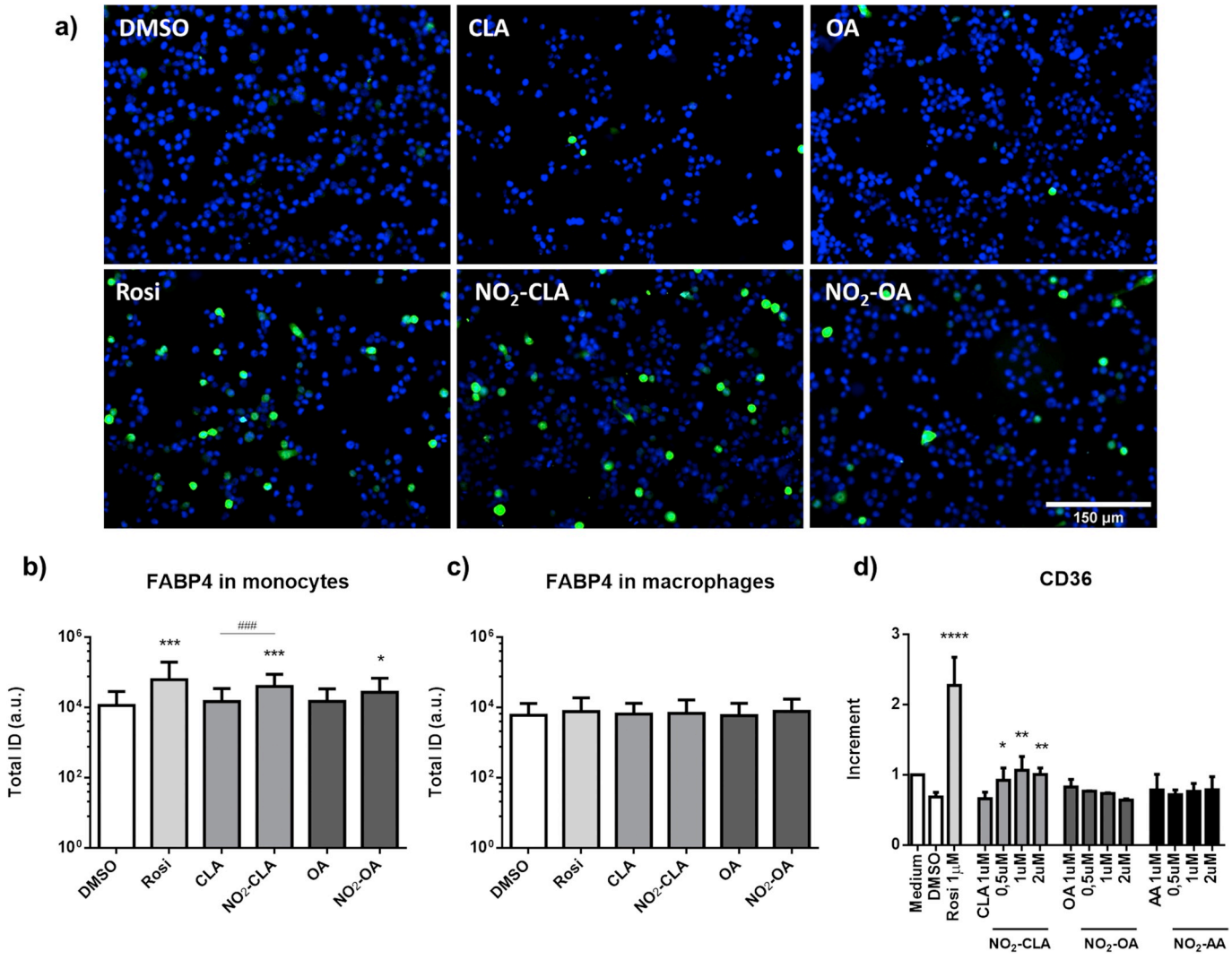

Fig. 2. NO_2-FA induced an increase in FABP4 and CD36 protein expression **in differentiating monocytes, but not in macrophages.**
Differentiating THP-1 monocytes **(a, b, d)** and THP-1 macrophages **(c)**, obtained by treatment with PMA, were stimulated with 1 µM concentration of Rosi, NO_2-FA or their corresponding FA precursors, or the concentration indicated in the figure. In parallel, cells were incubated with DMSO (vehicle) as a control. After 12 h stimulation, cells were washed and stained using affinity-purified rabbit anti-rFABP4 antibodies and Alexa488 conjugated anti-rabbit IgG for development. Nuclei were stained using DAPI. Cells were observed and counted using epifluorescence microscopy. Images were analyzed using Image J software. In **(a)**, panels show representative images of differentiating monocytes following incubation with the indicated stimuli or control. Graphs in **(b)** and **(c)** correspond to the quantification of FABP4 protein levels in differentiating monocytes and macrophages, respectively. Graphs indicate the Integrated Density (ID, in arbitrary units) for at least 70 cells per treatment ± SD. (*) and (#) Indicate statistically significant differences compared with DMSO or their non-nitrated precursor, respectively (One-way ANOVA, Dunn's Multiple Comparison test */#$p^{<}$0.05, ***/###$p^{<}$0.001). In **(d)** treatments were carried out for 16 h, then cells were harvested, and CD36 protein levels were determined by flow cytometry using a mouse IgM anti-human CD36 antibody and a phycoerythrin-conjugated anti-murine IgM for development. Graph represents protein levels normalized to Medium group, and are the mean of three independent experiments ± SD. (*) Indicates statistically significant differences compared with DMSO (Two-way ANOVA, Tukey's Multiple Comparison test * $p^{<}$0.05, **$p^{<}$0.01, ***$p^{<}$0.001, ****$p^{<}$0.0001).

monocytes (Fig. 3a and b, respectively). Similarly, analysis of FABP4 levels in cell extracts by Western blot (Fig. 3c) showed that GW9662 caused a reduction in FABP4 protein levels induced by Rosi (80% inhibition) or NO_2-FA (72 to 89% inhibition, Fig. 3d). Altogether, these results indicate that NO_2-FA activated PPARγ in differentiating monocytes. Moreover, NO_2-FA effects on *FABP4* and *CD36* expression were much lower than those induced by Rosi, supporting the partial PPARγ agonist actions of nitroalkenes, in agreement with previous studies using transfected cell lines [25].

3.2. FA nitration did not abrogate FABP4 binding

The induction of FABP4 synthesis by NO_2-FA might influence their own intracellular transport and signaling because FABP4 is the main FABP isoform involved in intracellular FA transport in monocytes and macrophages. Nonetheless, the role of NO_2-FA binding to FABPs is unknown, thus we hypothesized that the presence of a nitro group on the fatty acyl chain might modify FA interactions with FABP4. Therefore, we studied NO_2-FA binding to FABP4 *in vitro* using a competitive fluorescent binding assay based on the displacement of a fluorescent hydrophobic probe (ANS), previously bound to FABP4. For this assay, we used delipidated murine rFABP4 as a model, recognizing that FABP4 is highly conserved among mammals, with murine and human FABP4 sharing a high level of primary and secondary structure identity (both higher than 91%, Supplementary Fig. 6). The addition of increasing amounts of NO_2-FA to rFABP4 bound to ANS (at saturation conditions induced by a protein to probe molar ratio of 1:3) caused a progressive decrease in fluorescence, indicating the displacement of ANS from rFABP4 (Fig. 4). Displacement curves were adjusted to a hyperbolic decay, suggesting a 1:1 FABP4:NO_2-FA stoichiometry ratio

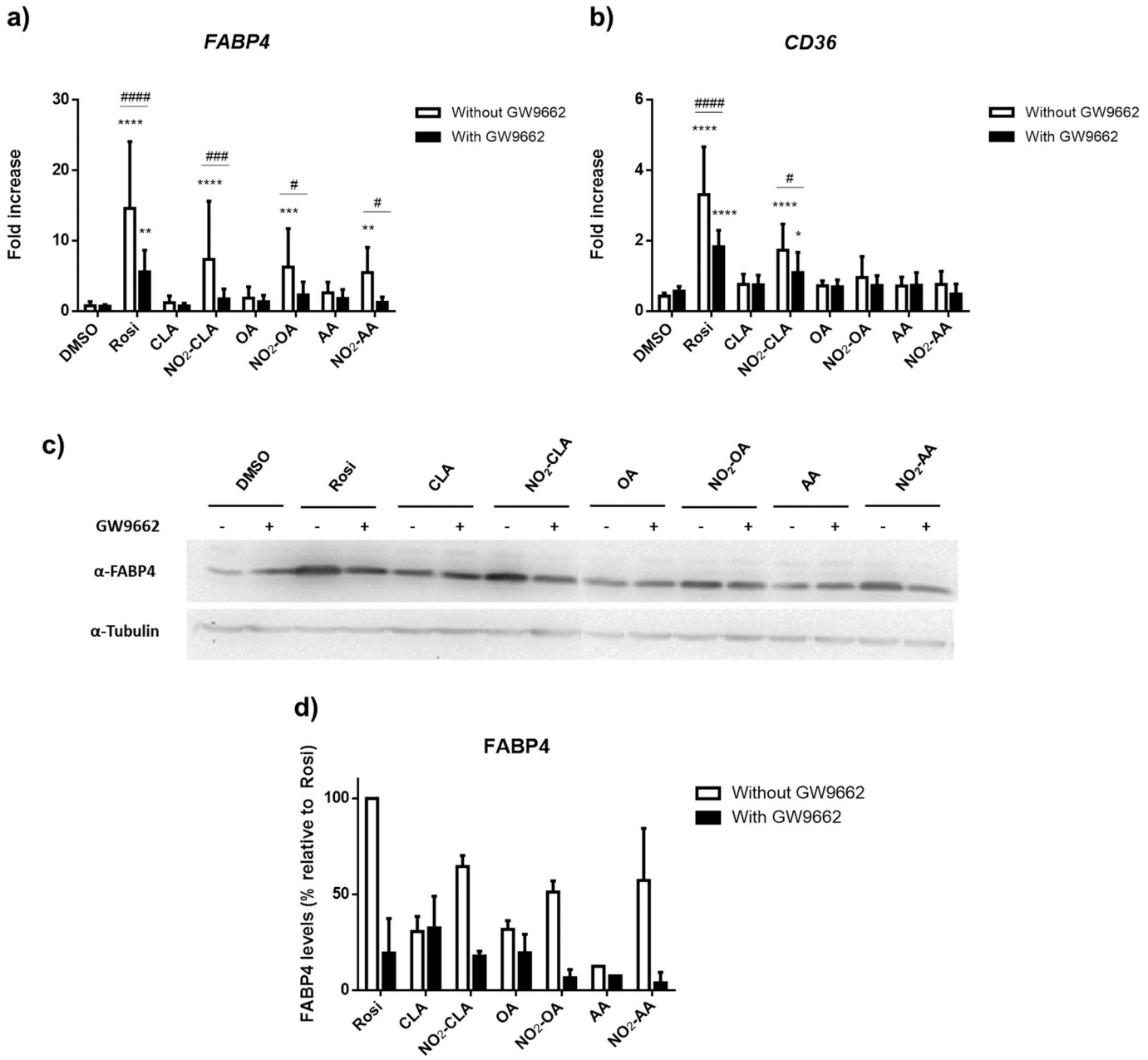

Fig. 3. Upregulation of *FABP4* and *CD36* expression by NO_2-FA was abolished by a PPARγ specific inhibitor.
Differentiating monocytes were pretreated with the PPARγ specific inhibitor GW9662 (1 μM) for 30 min and afterward, Rosi, NO_2-FA and their controls (DMSO and non-nitrated FA) were added at 1 μM to the culture. After 6 h post-stimulation, cells were homogenized to preserve total mRNA, and *FABP4* and *CD36* mRNA were measured by real-time qPCR and normalized to the housekeeping gene *GAPDH*. The expression of *FABP4* **(a)** and *CD36* **(b)** is represented as relative mRNA levels (fold increase) referred to Medium group (not shown), and correspond to the mean of three independent experiments ± SD. (*) and (#) Indicate statistically significant differences with DMSO or GW9662 treatment, respectively (Two-way ANOVA, Tukey's Multiple Comparison test */#$p^{<}$0.05, **/##$p^{<}$0.01, ***/###$p^{<}$0.001, ****/####$p^{<}$0.001). After 16 h stimulation, GW9662 effects on *FABP4* upregulation by NO_2-FA were examined at the protein level by Western Blot using α-tubulin as loading control; a representative Western blot result is shown in **(c)**, where two separate membranes from the same experiment were placed next to each other. FABP4 protein levels were quantified by densitometry of Western blot bands from three independent experiments and normalized to Rosi. The relative induction of FABP4 protein levels is shown in **(d)**.

in agreement with previous reports [56,57], and allowed K_{dapp} calculation. Differences in binding affinity among NO_2-FA were noted. NO_2-OA behaved like a high-affinity ligand, whereas NO_2-CLA and NO_2-AA acted as weak affinity ligands since they displaced about 84%, 58%, and 46% of ANS at protein saturation condition, respectively [48]. This correlated with the fact that NO_2-OA showed the lowest K_{dapp} (Table 2, indicated with *). On the other hand, according to $K_{dapp,}$ nitration of OA, CLA and AA caused a reduction in their rFABP4 affinity (Table 2, indicated with #), related to variations in binding free-energies of 0.27, 1.376 and 1.47 kcal mol^{-1} for each mixture of NO_2-OA, NO_2-CLA and NO_2-AA regioisomers, respectively. Despite such variations, acyl chain nitration did not abrogate FA binding to FABP4, supporting the idea that FABP4 could also act as a NO_2-FA intracellular carrier.

The *in silico* results show that FABP4-bound FA/NO_2-FA remained thermodynamically stable throughout the 1.2 μs simulation periods (Table 2, right) as previously reported for other 1:1 complexes established between murine FABP4 and different ligands [49,58–60]. The corresponding binding free-energies extracted from MM/GB(PB)SA

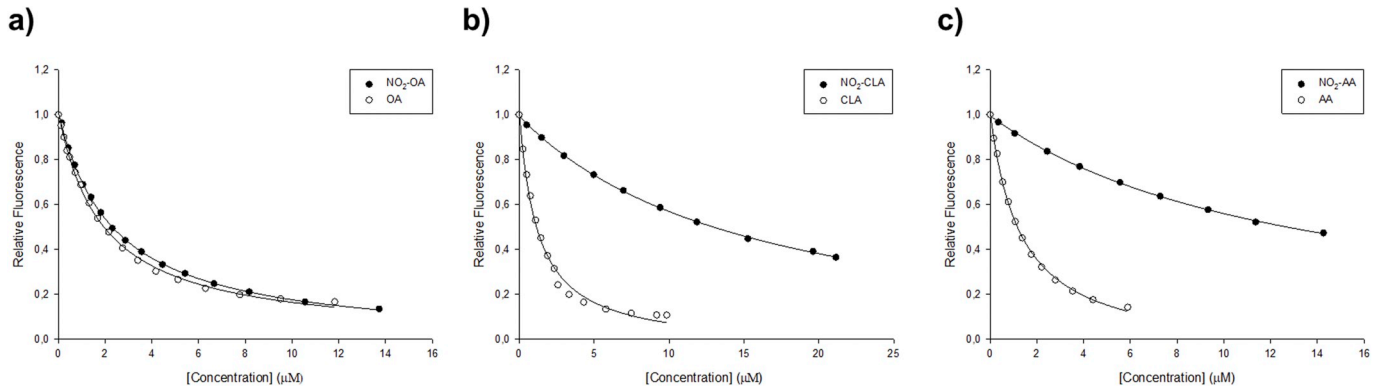

Fig. 4. ANS displacement from rFABP4 by NO_2-FA.
rFABP4 was loaded with ANS, and FA or NO_2-FA were added progressively, registering the emission spectrum of ANS after each addition. The increment in FA or NO_2-FA concentration induced a decrease in ANS fluorescence intensity. Each point corresponds to the integral of the ANS emission spectra at the indicated ligand concentration, and the line represents the adjustment to a hyperbolic decay. ANS displacements induced by FA (open circles) or NO_2-FA (filled circles) are shown for OA/NO_2-OA **(a)**, CLA/NO_2-CLA **(b)**, AA/NO_2-AA **(c)**. Curves are representative of three independent experiments.

Table 2
K_{dapp} and binding free energies at 298 K for murine FABP4:FA and FABP4:NO_2-FA (1:1 complexes).

Ligand	*In vitro* (rFABP4)		*In silico* murine FABP4 ΔG_{bind} (kcal mol^{-1})	
	K_{dapp} (μM)[a, b]	ΔG_{bind}[c] (kcal mol^{-1})	MMGBSA	MMPBSA
OA	0.59 ± 0.20	−8.49 ± 0.34	−41 ± 5	−41 ± 9
9-NO_2-OA	0.93 ± 0.16$^{\#\#e}$	−8.22 ± 0.17	−48 ± 5	−49 ± 8
10-NO_2-OA			−49 ± 5	−49 ± 9
CLA	0.28 ± 0.03	−8.90 ± 0.11	−42 ± 6	−44 ± 7
9-NO_2-CLA	3.03 ± 0.01$^{****/\#\#\#\#e}$	−7.524 ± 0.003	−49 ± 5	−49 ± 7
12-NO_2-CLA			−45 ± 5	−46 ± 8
AA	0.25 ± 0.02	−9.00 ± 0.08	n/a[d]	n/a[d]
NO_2-AA	3.02 ± 0.08$^{****/\#\#\#\#}$	−7.53 ± 0.03	n/a[d]	n/a[d]

[a] Values correspond to the mean of three independent experiments ± SD, determined by ANS displacement experiments using each NO_2-FA regioisomeric mixture or the corresponding FA precursor.
[b] The ($^{\#}$) and (*) superscripts indicate significant differences with respect to the corresponding FA precursor or NO_2-OA, respectively (One-way ANOVA, Tukey multiple comparison test $*/\#p^{<}0.05$, $**/\#\#p^{<}0.01$, $***/\#\#\#p^{<}0.001$).
[c] ΔG_{bind} = -RTln$K_{d\text{-}app}$ at T = 298 K.
[d] n/a: data not available, AA/NO_2-AA complexes were not simulated.
[e] Corresponding to the mixture of positional isomers.

calculations also enabled the evaluation of ligand affinities between regioisomers of NO_2-OA and NO_2-CLA (not assessed *in vitro*), without significant changes between isomers. These results provide further support that nitration did not compromise FA binding to FABP4.

3.3. FABP4 nuclear import occurs independently of NO_2-FA stimulation in differentiating monocytes

NO_2-FA promotion of FABP4 translocation into the nucleus was examined in differentiating monocytes, since this translocation has been correlated with PPARγ activation by synthetic agonists [61,62]. FABP4 translocation has been previously analyzed using artificial systems, where FABP4 was overexpressed in non-myeloid cell lines [63] or expressed as a fusion protein with GFP, which likely interferes with the ability of FABP4 to freely diffuse across the nuclear membrane [59,61,62]. To avoid this interference, studies were performed by confocal immunofluorescence microscopy using immunoaffinity-purified anti-rFABP4 antibodies for detection. FABP4 localization was first examined in differentiating monocytes stimulated with PMA plus NO_2-FA for 10 h in order to achieve a detectable FABP4 signal (FABP4 levels were very low in the absence of a PPARγ agonist, Fig. 2). FABP4 was equally distributed throughout the cell, showing a nucleus to cytoplasm ratio (N/T-N) of around 1 (Fig. 5a). Then, the effect of re-stimulation with Rosi, NO_2-FA or FAs on FABP4 localization was assessed after 30 or 60 min, as previously described for other ligands [62]. There were no significant changes in FABP4 nuclear transport in differentiating monocytes treated with a range of NO_2-FA and Rosi concentrations (1–10 μM) (Fig. 5b–e). In these assay conditions, total FABP4 levels in treated and control cells were comparable, indicating that re-stimulation did not induce FABP4 synthesis, which might have contributed to the cytoplasmic signal (Fig. 5f).

In addition to FABP4 diffusion into the nucleus as a small protein, nuclear translocation could also depend on the presence of an atypical, and undetectable from inspection of the linear sequence, nuclear localization signal (NLS) in the three-dimensional structure of FABP4. This is constituted by three basic residues (Lys21, Arg30, and Lys31) [62]. The NLS is exposed in FABP4 by conformational changes induced upon binding of an activating ligand, thus promoting a transition from an inactive (open) to an active (closed) portal conformation. This is characterized by the Phe57 pointing inwards and pushing outwards the *αI-loop-αII* cap [53]. Because NO_2-FA did not promote FABP4 nuclear translocation in our cell model, we explored through molecular dynamics simulations whether NO_2-FA and their corresponding native FA precursors would facilitate NLS exposition. In agreement with previous observations [60], the dynamics of the apo-FABP4 showed the presence of both open and closed portal conformations, with the majority of the population in the latter (76%, Table 3). Similarly, all FABP4:FA and FABP4:NO_2-FA complexes, showed both open and closed conformations

of FABP4, but there were differences in the percentage of structures exhibiting the closed conformation within the spectrum of conformations adopted by the protein. CLA and OA binding to FABP4 promoted a redistribution of the native population, favoring the closed portal conformation that exposes the NLS region (Fig. 5g and h and Table 3). In contrast, NO_2-FA binding showed dissimilar effects (Table 3). Binding of 10-NO_2-OA, but not of 9-NO_2-OA, enhanced the predominance of the Phe57 closed portal conformation to a similar extent as OA. On the other hand, 9- and 12-NO_2-CLA binding to FABP4 did not increase the predominance of the closed conformation as FA and 10-NO_2-OA did. Overall, these results indicated that NO_2-FA are not better inducers of an active/closed FABP4 conformation than their

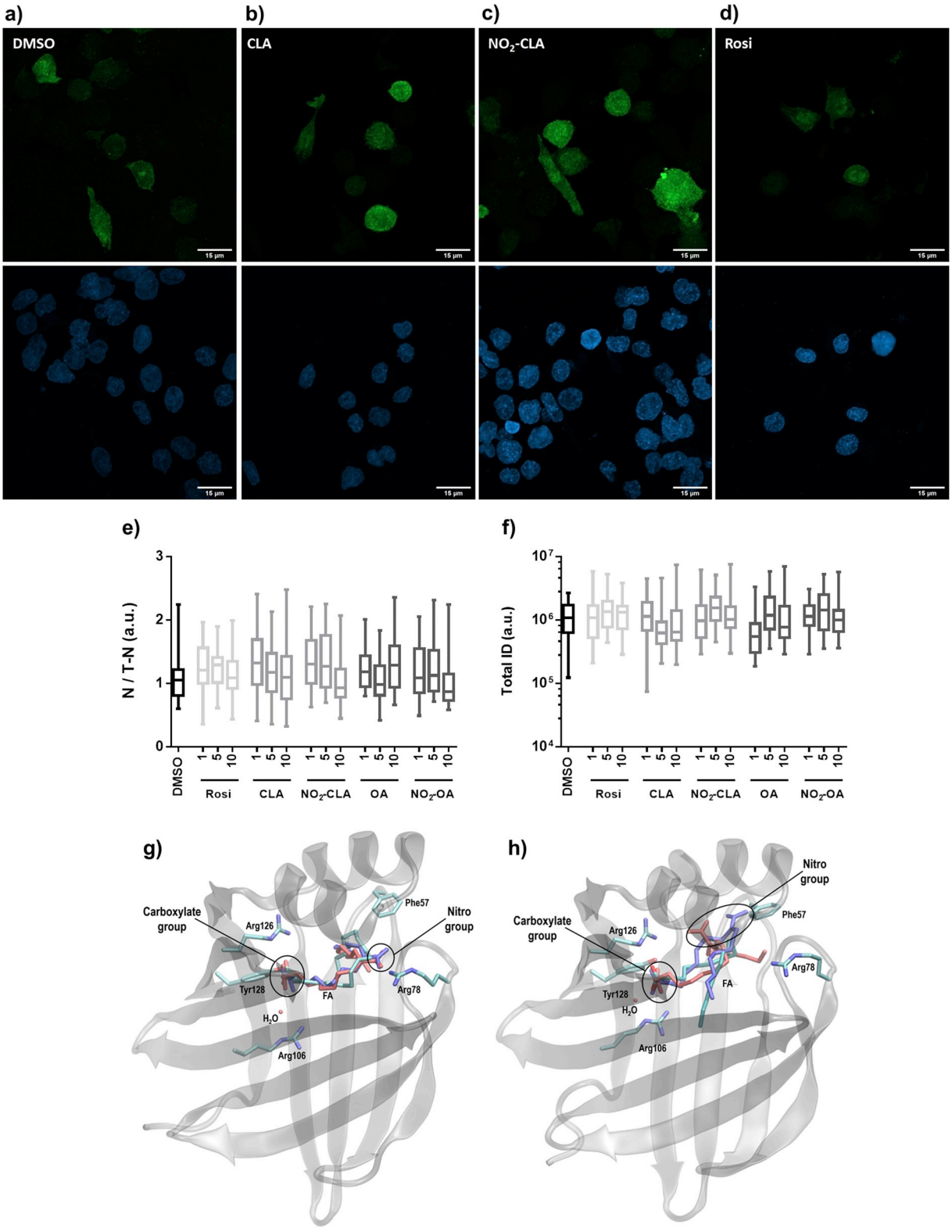

(caption on next page)

Fig. 5. NO_2-FA did not increase FABP4 nuclear localization in differentiating monocytes.
(a-f) Differentiating THP-1 monocytes obtained by treatment with PMA were stimulated with 1 μM concentration of NO_2-FA for 10 h and then treated with LMB (10 ng/ml) and re-stimulated with Rosi, NO_2-FA or their corresponding FA precursors in a range of concentrations (1–10 μM). In parallel, cells were re-stimulated with DMSO (vehicle) as a control. After 30 min of re-stimulation, cells were washed and stained using affinity purified rabbit anti-rFABP4 or control antibodies, and Alexa488 conjugated anti-rabbit IgG for development. Nuclei were stained using DAPI. Cells were observed and counted using confocal microscopy. Images were analyzed using Image J software. Magnification (63x) of representative FABP4 distribution in cells treated with DMSO **(a),** CLA **(b)**, NO_2-CLA **(c)**, or Rosi **(d)**. Quantification of the intracellular distribution calculated as the ratio Nuclear ID/(Total ID-Nuclear ID) (N/T-N) **(e)** and total integrated density **(f)** after 30 min of re-stimulation. Plots showed box and whisker with bars from minimum to maximum value corresponding to the quantification of at least 30 cells per condition. Results are representative from three independent experiments. **(g)** and **(h)** Superimposed representative structures for the most populated conformation corresponding to a closed portal (NLS exposed), for each FA or NO_2-FA, 1:1 complexes with murine FABP4 (backbone in grey) from MD simulations. Phe57 and key residues interacting with polar heads in FA (carboxylate) and NO_2-FA (carboxylate and NO_2) are evidenced in stick representation. **(g)** OA series: OA, 9-NO_2-OA and 10-NO_2-OA ligands in cyan, violet and red, respectively. **(h)** CLA series: CLA, 9 NO_2-CLA and 12-NO_2-CLA ligands in cyan, violet and red, respectively. (For interpretation of the references to colour in this figure legend, the reader is referred to the Web version of this article.)

Table 3
Relative weight of closed portal conformations (expressed in percentage) from FABP4:FA and FABP4:NO_2-FA complexes 1.2 μs molecular dynamics simulations.

Ligand	FABP4:ligand complexes (1:1) closed portal conformation (%)
OA	87
9-NO_2-OA	71
10-NO_2-OA	87
CLA	91
9-NO_2-CLA	71
12-NO_2-CLA	66
No ligand	76[a]

[a] Previously reported as 62% by Li et al. [60] using a different Amber2012 force field (ff03) for protein simulation.

corresponding FA precursors.

3.4. FABP4 transduces NO_2-FA signaling

Evaluation of FABP4 involvement in cell signaling by NO_2-FA in differentiating monocytes was performed using the FABP4 inhibitors BMS and HTS, which have higher affinities for FABP4 than NO_2-FA [42,43]. Monocytes were differentiated in the presence of FABP4 inhibitors and afterward, cells were stimulated with NO_2-FA or native FA as control, and *FABP4* and *CD36* expression followed to indicate PPARγ activation. In these assays, inhibitors did not affect basal levels of FABP4 (Supplementary Fig. 7). BMS treatment caused a reduction in the upregulation of *FABP4* expression induced by NO_2-FA and abrogated the *CD36* expression induced by NO_2-CLA (Fig. 6a and b). These results were similarly reproduced by HTS, which strongly inhibited *FABP4* and *CD36* expression by NO_2-FA (Fig. 6c and d). Then, we examined the effect of FABP4 inhibitors on the NO_2-FA-dependent induction of *HMOX1*, *GCLM,* and *HSP70* expression. We found that BMS treatment elicited different effects on NO_2-OA and NO_2-CLA signaling. NO_2-OA induced significant increases in both *HMOX1* and *GCLM* expression that were partially or completely inhibited by BMS, respectively (Fig. 6e and f). In contrast, NO_2-CLA caused a modest upregulation of *HMOX1* expression that was not inhibited by BMS treatment (Fig. 6e). Analysis of NO_2-FA activation of the HSF1 signaling showed that NO_2-OA, but not NO_2-CLA, upregulated *HSP70* expression, which was significantly reduced by BMS (Fig. 6g). In contrast, when the effect of HTS was assessed on Keap1/Nrf2 and HSF1 reporter gene expression, a significant increase in mRNA levels of target genes was observed, which impeded a direct comparison of gene expression between control and treated cells. Despite this effect, normalization of gene expression by their corresponding basal levels revealed that HTS and BMS induced comparable inhibitory effects on NO_2-FA-induced activation of Keap1/Nrf2 (Supplementary Fig. 8).

3.5. FABP4 regulates NO_2-FA modulation of cytokine expression

Cytokine expression is a feature of the inflammatory profile of monocytes and macrophages, which is known to be modulated by NO_2-FA. Since PPARγ modulates inflammatory responses, we explored whether activation of the PPARγ/FABP4 axis might influence cytokine expression by differentiating monocytes. To that end, we determined *MCP1* and *IL1B* expression in the presence or absence of GW9662 or BMS. NO_2-OA inhibited *MCP1* and *IL1B* expression (Fig. 7a and d), while NO_2-CLA had a marginal effect on *MCP1*. Moreover, considering that GW9662 did not modify NO_2-OA effects, activation of PPARγ is likely not involved in NO_2-OA modulation of cytokine expression. Although PPARγ does not mitigate these anti-inflammatory effects, FABP4 does, since NO_2-OA effects on *MCP1* and *IL1B* were inhibited by FABP4 blockade (around a 87% and 44%, respectively).

4. Discussion

The pleiotropic anti-oxidant and anti-inflammatory actions of NO_2-FA have led to the present evaluation of these species as new drug candidates designed to alleviate disorders in which physiological regulatory circuits intended to control inflammation fail [30,64]. *In vivo* studies in various pre-clinical inflammatory models support this possibility [65]. Despite the considerable past and current understanding of NO_2-FA actions in modulating inflammatory responses, these mostly focused on those regulated by NF-κB and Nrf2 [27–29,66]. At present there is limited insight into the ability of NO_2-FA to activate PPARγ in macrophages and differentiating monocytes [10,36].

We found that NO_2-FA, but not native FA at similarly low concentrations, induced PPARγ activation in differentiating monocytes and macrophages, reinforcing the unique impact of the electrophilic character imparted by unsaturated FA nitration. While non-physiological concentrations of native FA activate PPARγ (around 100 μM *in vitro)* [67,68], several characteristics differentiate the activity exerted by NO_2-FA from native FA. NO_2-FA, are orders of magnitude more potent activators than native FA, but are present at orders of magnitude lower concentrations, making comparisons challenging. Importantly, by reacting covalently, NO_2-FA have much longer occupancy times that are determined by the rate of the elimination reaction or protein turnover as opposed to the pharmacokinetic properties of native FAs. In addition, while NO_2-FA can compete with FA for ligand binding domain association, FAs will not be able to compete with adducted NO_2-FA, thus intracellular levels of NO_2-FA become less relevant for initiating and sustaining an activated state of the receptor.

Plasma levels of NO_2-FA are in the very low nM range [6,9], with net intracellular concentrations difficult to estimate as NO_2-FA are found esterified in complex lipids and covalently bound to proteins, small thiols, and other nucleophilic intracellular molecules [69]. Thus, the free acid fraction of NO_2-FA, while in equilibrium with these other components, is viewed to be a minor percentage [70]. Regarding intracellular concentrations of free FAs, limited data has been reported for monocytes and macrophages, with one report indicating at least 1 μmol/10^6 THP-1 cells [71]. In any case, in our assays 10^6 THP-1 cells were treated with 2 nmoles of NO_2-FA, a level orders of magnitude lower than native FA levels, affirming that NO_2-FA exert effects even

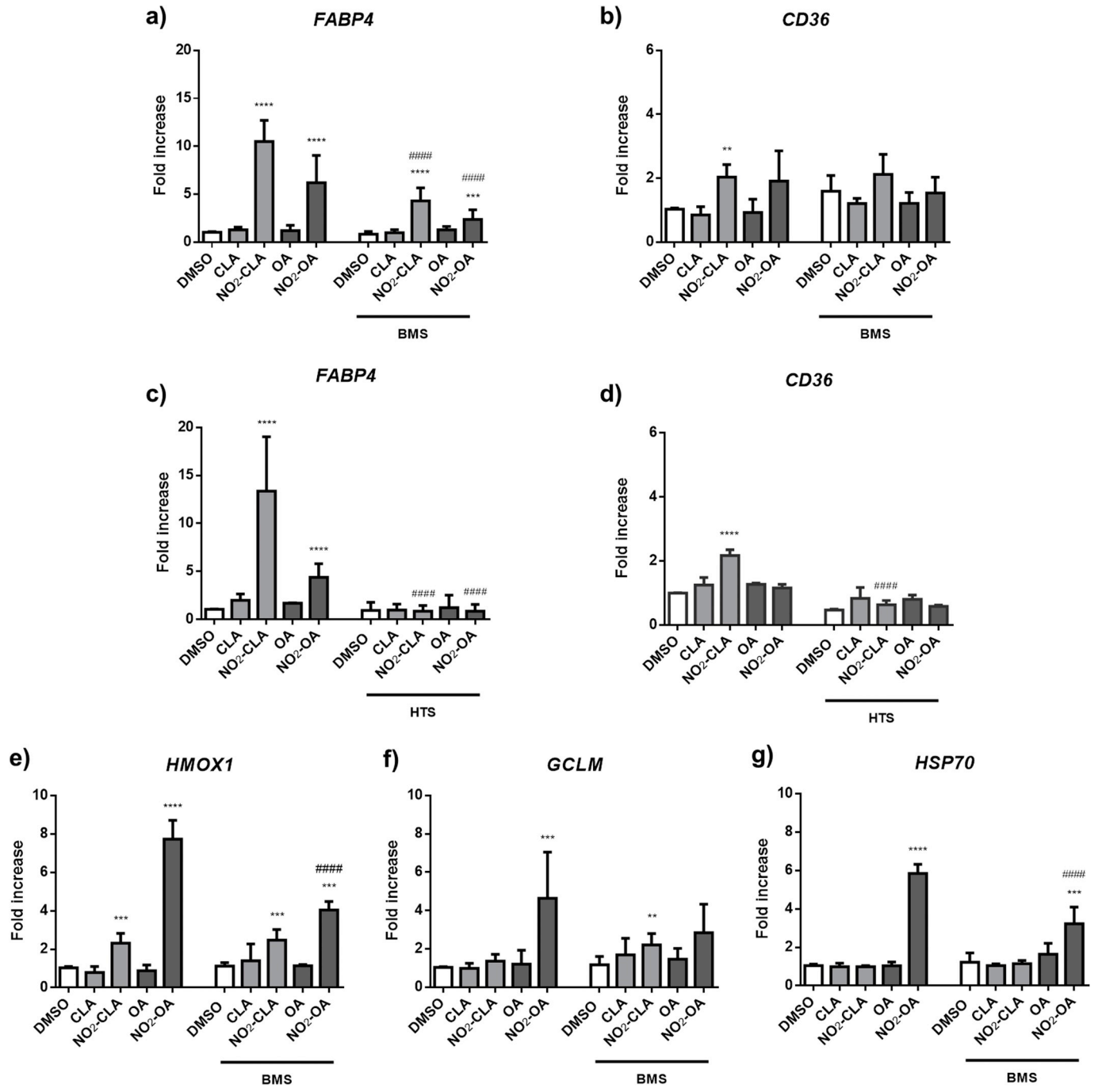

Fig. 6. Blocking FABP4 binding activity inhibits **NO_2-FA activation of PPARγ, Keap1/Nrf2 and HSF1 in differentiating monocytes.**
(a-g) THP-1 cells were differentiated with PMA in the presence of the FABP4 inhibitor BMS (25 μM)/HTS (15 μM) or DMSO (control) for 2 h. Then, NO_2-FA (1 μM) or DMSO as control were added for 6 h. To examine NO_2-FA signaling actions, total mRNA was purified and *FABP4* **(a and c)**, *CD36* **(b and d),** *HMOX1* **(e)**, *GCLM* **(f)**, or *HSP70* **(g)** expression, by real-time qPCR. Results are represented as relative mRNA levels (fold increase) referred to DMSO group and correspond to the mean of four independent experiments ± SD. (*) Indicates statistically significant differences with the corresponding control (DMSO or DMSO + BMS/DMSO + HTS, Two-way ANOVA, Tukey's Multiple Comparison test * $p<0.05$, ** $p<0.01$, *** $p<0.001$, **** $p<0.001$). (#) Indicates statistically significant differences with the same treatment without inhibitor (Two-way ANOVA, Tukey's Multiple Comparison test #$p<0.05$, ##$p<0.01$, ###$p<0.001$, ####$p<0.001$).

when native FA are in excess. Extents of PPARγ activation by NO_2-FA were lower in macrophages, yet there were no changes in *PPARG* expression levels found between differentiating monocytes and macrophages. The transcriptomic profile of human monocytes undergoes alterations during differentiation towards macrophages, which include the induction of transcripts involved in palmitate and oleate synthesis, as well as in fatty acid desaturation and elongation, leading to differences in the lipidomic profile [72]. In this scenario, the lower ability of NO_2-FA to activate PPARγ in macrophages may be associated with the presence of higher-affinity and/or higher concentrations of competing endogenous ligands in this cell type, which might render NO_2-FA less effective in PPARγ activation. In line with this hypothesis, basal PPARγ activation, measured in terms of *FABP4* mRNA levels, seems to be much greater in macrophages than in monocytes (around 16-fold, Supplementary Fig. 9).

NO_2-FA acted as partial PPARγ agonists in monocyte and

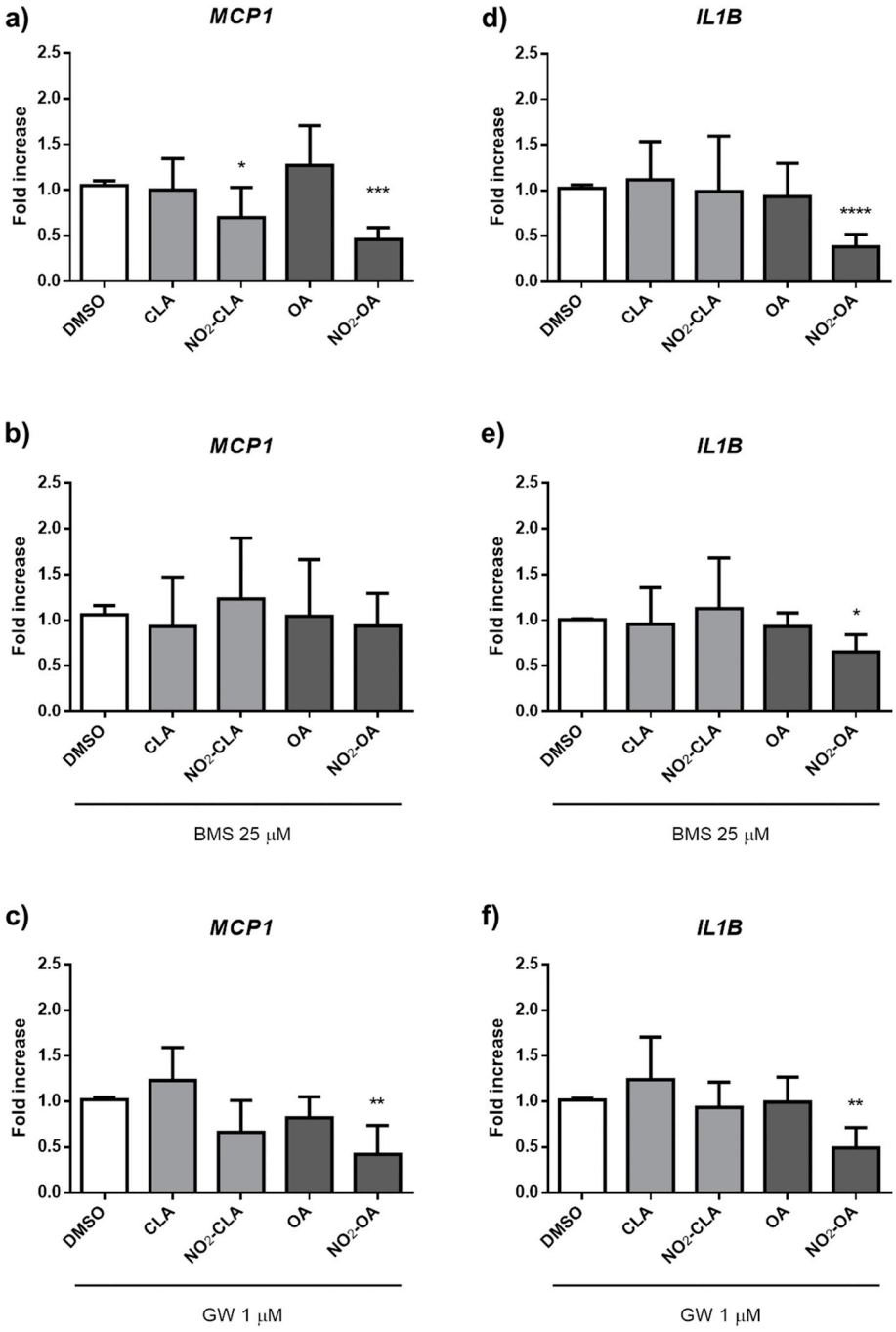

Fig. 7. FABP4 modulates **NO_2-FA** inhibition **of cytokine expression**.
Differentiating THP-1 monocytes obtained by treatment with PMA were stimulated with 1 μM concentration of Rosi, NO_2-FA or their corresponding FA precursors **(a–f)**. In parallel, cells were incubated with DMSO (vehicle) as a control. After 6 h stimulation, cells were homogenized to obtain total mRNA and *MCP1 and IL1β* mRNA levels were determined by real-time-qPCR and normalized to the housekeeping genes *GAPDH* or *18S*. For BMS experiments, THP-1 cells were differentiated with PMA in the presence of the FABP4 inhibitor BMS (25 μM) for 2 h previous to NO_2-FA treatment **(b)** and **(e)**. For GW9662 experiments, differentiating monocytes were pretreated with GW9662 (1 μM) for 30 min previous to NO_2-FA treatment **(c)** and **(f)**. The expression of *MCP1* **(a–c)** and *IL1β* **(d–f)** is represented as relative mRNA levels (fold increase) referred to DMSO, and correspond to the mean of three independent experiments ± SD. (*) Indicates statistically significant differences with DMSO/DMSO + BMS/DMSO + GW9662 treatment (Two-way ANOVA, Tukey's Multiple Comparison test *$p<0.05$, **$p<0.01$, ***$p<0.001$, ****$p<0.001$).

macrophages, a result consistent with previous studies using biochemical approaches and transfected cell lines. In all conditions and for all reporter genes measured, the full PPARγ agonist Rosi caused a stronger activation than NO_2-OA and NO_2-CLA. This behavior is likely associated with less displacement of co-repressors and lower recruitment of co-activators in comparison with Rosi, as previously reported for NO_2-OA [25]. Considering the potential use of NO_2-OA as an anti-inflammatory drug, this feature is not a disadvantage, as partial agonists of PPARγ that discriminate between the beneficial actions and the adverse effects associated with full PPARγ activation may be of clinical benefit. Thiazolidinedione-related increases in cardiovascular events led to both market withdrawal and a restricted use in several countries [34]. In this regard, understanding the differences observed in the potency and transcriptional output of distinct NO_2-FA, can help explain the molecular events leading to the beneficial and/or undesirable effects triggered by PPARγ activation. Moreover,particular NO_2-FA regiosiomers may undergo different interactions with this nuclear receptor [22,23]).

Among NO_2-FA, NO_2-CLA induced a greater magnitude of PPARγ activation, as shown by its unique upregulation of *CD36* expression, a response inhibited by GW9662. This expands our knowledge of the biological actions of NO_2-CLA in monocytes and macrophages and presumably other cells [5,17,73,74]. Because CLA behaves as a preferential FA target for nitration at physiological conditions [5], PPARγ activation by NO_2-CLA could be biologically more relevant than that mediated by other NO_2-FA. However, whether NO_2-CLA plays a role as an endogenous PPARγ agonist and physiological regulator is still controversial since NO_2-CLA levels in inflamed fluids or specific anatomic compartments of tissues from patients with acute or chronic inflammatory diseases are unknown. In a mouse peritonitis model, NO_2-

CLA levels were ~20 nM in peritoneal lavage, indicating ~μM concentrations in undiluted native peritoneal fluid, as there is a limited recovery of this chemically-reactive lipid from the peritoneal cavity because of alternative reactions [17].

FABP4, the most highly upregulated PPARγ-reporter gene in response to NO_2-FA treatment, is a lipid carrier which binds and delivers ligands to PPARγ [61–63,75]. FABP4 binds a series of NO_2-FA with an affinity similar or lower than that corresponding to native FA precursors, but in the intracellular milieu, this binding would depend on the concentration of FABP4, NO_2-FA as well as other competing FA ligands. On the other hand, the NO_2-FA binding affinity for FABP4 did not correlate with an ability to activate PPARγ, since NO_2-OA showed the highest FABP4 binding affinity (Table 2), but not the strongest PPARγ activation activity among NO_2-FA. Upon ligand binding, FABP4 undergoes structural changes, adopting the closed/active conformation that promotes nuclear translocation and, in turn, PPARγ activation. Thus, we compared the degree of FABP4 nuclear translocation induced by NO_2-FA and corresponding native FA precursors. In our experimental conditions, FABP4 nuclear translocation was similar in differentiating monocytes stimulated with NO_2-FA or FA precursor. Furthermore, molecular simulations showed that the closed/active conformation of FABP4 is present in the dynamics of both FABP4:FA and FABP4:NO_2-FA complexes as in the apo-FABP4. This agrees with the precept that in all assay conditions at least half of total FABP4 was present in the nucleus (Fig. 5). Taking into account the unique nature of NO_2-FA-FABP4 interactions, NO_2-FA seem not to play a major role in stabilizing the active FABP4 conformation. However, NO_2-FA-mediated FABP4 translocation might be difficult to detect, considering that, as discussed above, in the cellular milieu NO_2-FA must compete with relatively higher concentrations of endogenous FA, and NO_2-FA-FABP4 complexes are not more active in terms of nuclear translocation. Importantly, the lack of correlation between the binding affinity of NO_2-FA for FABP4 and the strength of the PPARγ activation response does not exclude the involvement of FABP4 in the mechanism of PPARγ activation by NO_2-FA. FABP4 levels might be high enough to carry high -and low-affinity ligands, even those in low concentration such as NO_2-FA. Indeed, two different FABP4 inhibitors inhibited NO_2-FA-mediated PPARγ activation. In aggregate, this data reveals that PPARγ activation by NO_2-FA induces *FABP4* upregulation and thus instigates a positive amplification loop of this signaling pathway (Fig. 8).

Any differences in PPARγ activation by different NO_2-FA and FA could not be attributed to differences in NO_2-FA-FABP4 interactions, as nitration did not enhance FA binding to FABP4 or consequent FABP4 nuclear translocation. Therefore, it is more likely that nitration could modify the set of interactions that determine how the lipid acyl chain is accommodated in the ligand-binding domain (LBD) of PPARγ, thus influencing receptor conformation and activity. The chemical features of the ligand define the PPARγ-LBD structural changes that stabilize a particular receptor conformation and determine the position adopted by helix 12 and this domain's binding of co-activators and release of co-repressors [76]. In the case of NO_2-FA, the crystal structure of PPARγ complexed with two nitrolinoleic acid (NO_2-LA) regioisomers revealed that this nitroalkene establishes specific interactions with amino acids of the PPARγ binding pocket, which are not shared by the Rosi interaction network at the LBD, thus conferring partial agonism of transcriptional responses [24]. These unique events include interactions between the nitro group and Arg288 or Glu343, as well as interactions between Phe287 and the NO_2-LA backbone, required for stable binding of NO_2-LA. Furthermore, NO_2-FA interactions with PPARγ-LBD are further stabilized by the formation of a covalent bond with the redox-sensitive Cys285 in the LBD of PPARγ [25]. Consequently, differences in PPARγ activation by NO_2-CLA, NO_2-OA and NO_2-AA may be related to the set of non-covalent and covalent interactions that each nitroalkene establishes with the PPARγ-LBD, which in turn determine the complex stability and the degree of conformational changes induced by the occupancy of the ligand on the binding pocket and the downstream recruitment/release of coactivators and corepressors.

The potential of NO_2-FA to bind FABP4 and to upregulate *FABP4* expression might have additional implications for tissue NO_2-FA responses. To explore this, we took advantage of the ability of NO_2-FA to induce *HMOX1/GCLM* and *HSP70* expression via Keap1/Nrf2 and HSF1, respectively. In contrast with a modest relative activation of PPARγ, NO_2-OA was more active than NO_2-CLA. Using breast cancer cells, NO_2-OA elicited greater Nrf2 and lower PPARγ transcriptional activity responses than NO_2-LA [77]. Several factors might be involved in this differential potency for activating these signaling pathways. As noted for PPARγ, differences in the set of non-covalent/covalent bonds formed between NO_2-FA and the target protein could affect the strength of the signaling response. We speculate that for stress-induced transcriptional responses, differences related to NO_2-FA Michael addition kinetics and equilibrium constants with thiol targets may be more important, since this will affect thiol residency time, net populations of thiol targets and downstream propagation of the signal. These differences could also affect "signaling-productive" versus alternative NO_2-FA reactions, as this would impact the formation of adducts with thiol-bearing pools of molecules, including glutathione and proteins not involved in catalysis or the regulation of gene expression. In this context, the greater activity showed by NO_2-OA compared to NO_2-CLA might be

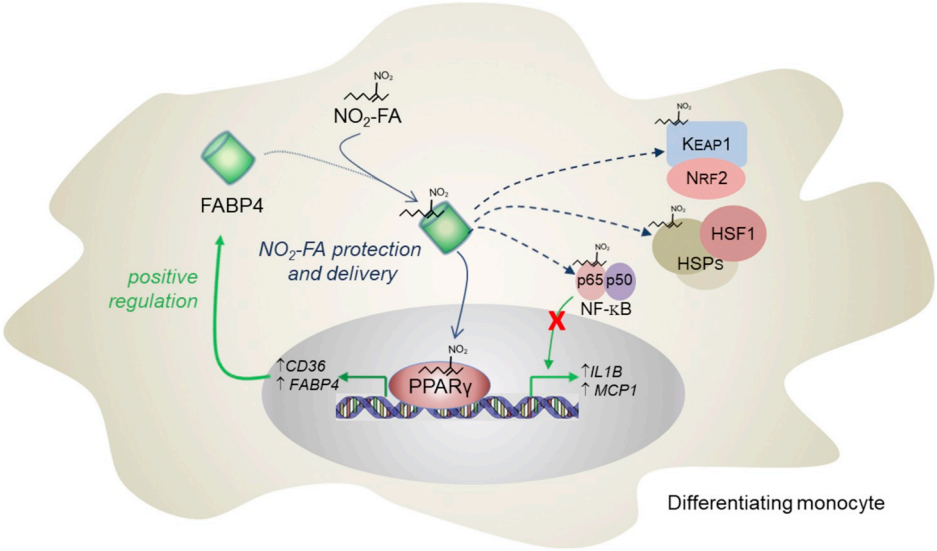

Fig. 8. Involvement of the FABP4/PPARγ signaling axis in differentiating monocyte NO_2-FA signaling.
NO_2-FA behave as potential ligands of FABP4. NO_2-FA binding to FABP4 may protect them from irrelevant adduction reactions favoring their interaction with factors involved in intracellular pathways associated with anti-oxidative and anti-inflammatory responses (Keap1/Nrf2, HSPs/HSF1, NF-κB). In addition, FABP4 is involved in the activation of PPARγ triggered by NO_2-FA, which likely includes the trafficking and delivery of these lipids to PPARγ. As a result of PPARγ activation, FABP4 expression is upregulated, which would operate as a positive regulation mechanism of the FABP4/PPARγ axis.

explained by the fact that in our assays, at the same molar concentration, NO_2-OA could react more rapidly with nucleophiles than NO_2-CLA [78]. When analyzing the involvement of FABP4 in NO_2-FA-induced signaling responses, FABP4 inhibitors in turn limited the *HMOX1* up-regulation induced by NO_2-OA, but not by NO_2-CLA. We envision that FABP4 could also limit NO_2-FA reaction with non-productive cellular nucleophiles such as glutathione, that in turn promotes cellular export of NO_2-FA-glutathione adducts [79]. Thus, the net effect of FABP4 sequestration would be to promote NO_2-FA reactions with more productive targets rather than inactivation and export.

Expanding the relevance of FABP4 in regulating NO_2-FA signaling, FABP4 inhibition attenuated NO_2-FA inhibition of pro-inflammatory cytokine expression in monocytes and macrophages. There was not a role for PPARγ in mediating these anti-inflammatory responses, suggesting that NF-κB transrepression by NO_2-FA-mediated PPARγ activation is less impactful than the inhibition of pro-inflammatory gene expression via the direct adduction of NF-κB p65 by NO_2-FA [10].

5. Conclusions

This work reveals that the lipid binding protein FABP4 is upregulated in monocytes in response to NO_2-FA mediated PPARγ activation. It also shows that FABP4 regulates NO_2-FA signaling through a chaperone function that probably improves the cellular transport of NO_2-FA and the downstream amplification of adaptive signaling responses. Upon induction of FABP4 expression by inflammatory stimuli and NO_2-FA-FABP4 binding, the expression of Nrf2 and HSF-1 regulated tissue-protective genes is enhanced and expression of pro-inflammatory cytokines is inhibited. These responses to NO_2-FA, all associated with inflammatory resolution and tissue repair [80–83] are facilitated by the chaperone activity of FABP4.

Funding

This work was supported by Comisión Sectorial de Investigación Científica (CSIC, Uruguay, grants Programa Iniciación a la Investigación C272 and Programa Grupos 536) and Agencia Nacional de Investigación e Innovación (ANII, Uruguay, fellowships to MLB) and National Institutes of Health (NIH, USA, grants R01GM125944 and R01DK112854 to FJS and grants P01HL103455 and R01HL132550 to BAF. JB, ELC, HR, and AMF are active members of the Sistema Nacional de Investigadores (SNI-ANII, Uruguay) and Programa de Desarrollo de las Ciencias Básicas (PEDECIBA Áreas Química y Biología, Uruguay), whose continuous support is gratefully acknowledged.

Declaration of competing interest

The authors declare the following financial interests/personal relationships which may be considered as potential competing interests: BAF and FJS acknowledge an interest in Complexa, Inc. and Creegh Pharmaceuticals.

Acknowledgments

Authors are grateful to Dra. Virginia López (Facultad de Química, UdelaR, Uruguay) for her assistance in the preparation of nitroarachidonic acid, Lic. Natalia Botasso (INIBIOLP, Argentina) for her help during the preparation of recombinant FABP4, and Andrés Di Paolo (Instituto de Investigaciones Biológicas Clemente Estable, Uruguay) for technical advice with confocal studies.

Appendix A. Supplementary data

Supplementary data to this article can be found online at https://doi.org/10.1016/j.redox.2019.101376.

References

[1] F.J. Schopfer, C. Cipollina, B.A. Freeman, Formation and signaling actions of electrophilic lipids, Chem. Rev. 111 (2011) 5997–6021.
[2] L. Villacorta, et al., Nitro-fatty acids in cardiovascular regulation and diseases: characteristics and molecular mechanisms, Front. Biosci. (2017) 873–889.
[3] W.A. Pryor, Free radical biology and medicine: it's a gas, man!, AJP Regul. Integr. Comp. Physiol. 291 (2006) R491–R511.
[4] R. Atkinson, S.M. Aschmann, A.M. Winer, J.N. Pitts, Gas phase reaction of NO2 with alkenes and dialkenes, Int. J. Chem. Kinet. 16 (1984) 697–706.
[5] G. Bonacci, et al., Conjugated linoleic acid is a preferential substrate for fatty acid nitration, J. Biol. Chem. 287 (2012) 44071–44082.
[6] M. Delmastro-Greenwood, et al., Nitrite and nitrate-dependent generation of anti-inflammatory fatty acid nitroalkenes, Free Radic. Biol. Med. 89 (2015) 333–341.
[7] D.A. Vitturi, et al., Convergence of biological nitration and nitrosation via symmetrical nitrous anhydride, Nat. Chem. Biol. 11 (2015) 504–510.
[8] V. Rudolph, et al., Endogenous generation and protective effects of nitro-fatty acids in a murine model of focal cardiac ischaemia and reperfusion, Cardiovasc. Res. 85 (2010).
[9] D. Tsikas, A.A. Zoerner, A. Mitschke, F.M. Gutzki, Nitro-fatty acids occur in human plasma in the picomolar range: a targeted nitro-lipidomics GC-MS/MS study, Lipids 44 (2009) 855–865.
[10] T. Cui, et al., Nitrated fatty acids: endogenous anti-inflammatory signaling mediators, J. Biol. Chem. 281 (2006).
[11] A. Trostchansky, et al., Synthesis, isomer characterization, and anti-inflammatory properties of nitroarachidonate, Biochemistry 46 (2007) 4645–4653.
[12] J. Hwang, K.E. Lee, J.Y. Lim, S.I. Park, Nitrated fatty acids prevent TNFα-stimulated inflammatory and atherogenic responses in endothelial cells, Biochem. Biophys. Res. Commun. 387 (2009) 633–640.
[13] T.K. Rudolph, et al., Nitro-fatty acids reduce atherosclerosis in apolipoprotein E-deficient mice, Arterioscler. Thromb. Vasc. Biol. 30 (2010) 938–945.
[14] L. González-Perilli, et al., Nitroarachidonic acid prevents NADPH oxidase assembly and superoxide radical production in activated macrophages, Free Radic. Biol. Med. 58 (2013) 126–133.
[15] L. Villacorta, et al., Electrophilic nitro-fatty acids inhibit vascular inflammation by disrupting LPS-dependent TLR4 signalling in lipid rafts, Cardiovasc. Res. 98 (2013) 116–124.
[16] L. González-Perilli, et al., Nitroarachidonic acid (NO2AA) inhibits protein disulfide isomerase (PDI) through reversible covalent adduct formation with critical cysteines, Biochim. Biophys. Acta Gen. Subj. 1861 (2017) 1131–1139.
[17] L. Villacorta, et al., In situ generation, metabolism and immunomodulatory signaling actions of nitro-conjugated linoleic acid in a murine model of inflammation, Redox Biol 15 (2018) 522–531.
[18] C. Batthyany, et al., Reversible post-translational modification of proteins by nitrated fatty acids in vivo, J. Biol. Chem. 281 (2006) 20450–20463.
[19] M. Lehrke, M.A. Lazar, The many faces of PPAR?? Cell 123 (2005) 993–999.
[20] L. la C. Poulsen, M. Siersbæk, S. Mandrup, PPARs: fatty acid sensors controlling metabolism, Semin. Cell Dev. Biol. 23 (2012) 631–639.
[21] F.J. Schopfer, et al., Nitrolinoleic acid: an endogenous peroxisome proliferator-activated receptor gamma ligand, Proc. Natl. Acad. Sci. U.S.A. 102 (2005) 2340–2345.
[22] M.J. Gorczynski, et al., Activation of peroxisome proliferator-activated receptor γ (PPARγ) by nitroalkene fatty acids: importance of nitration position and degree of unsaturation, J. Med. Chem. 52 (2009) 4631–4639.
[23] R.L. Alexander, et al., Differential potencies of naturally occurring regioisomers of nitrolinoleic acid in PPARγ activation, Biochemistry 48 (2009) 492–498.
[24] Y. Li, et al., Molecular recognition of nitrated fatty acids by PPAR gamma, Nat. Struct. Mol. Biol. 15 (2008) 865–867.
[25] F.J. Schopfer, et al., Covalent peroxisome proliferator-activated receptor γ adduction by nitro-fatty acids: selective ligand activity and anti-diabetic signaling actions, J. Biol. Chem. 285 (2010) 12321–12333.
[26] R.T. Nolte, et al., Ligand binding and co-activator assembly of the peroxisome proliferator- activated receptor-γ, Nature 395 (1998) 137–143.
[27] M.M. Wright, et al., Fatty acid transduction of nitric oxide signaling: nitrolinoleic acid potently activates endothelial heme oxygenase 1 expression, Proc. Natl. Acad. Sci. U.S.A. 103 (2006) 4299–4304.
[28] E. Kansanen, et al., Nrf2-dependent and -independent responses to nitro-fatty acids in human endothelial cells: identification of heat shock response as the major pathway activated by nitro-oleic acid, J. Biol. Chem. 284 (2009) 33233–33241.
[29] E. Kansanen, et al., Electrophilic nitro-fatty acids activate Nrf2 by a Keap1 cysteine 151-independent mechanism, J. Biol. Chem. 286 (2011) 14019–14027.
[30] A.J. Deen, et al., Regulation of stress signaling pathways by nitro-fatty acids, Nitric Oxide 78 (2018) 170–175.
[31] S. Yue, et al., The myeloid heat shock transcription factor 1/β-catenin axis regulates NLR family, pyrin domain-containing 3 inflammasome activation in mouse liver ischemia/reperfusion injury, Hepatology 64 (2016) 1683–1698.
[32] M. Shin, et al., Hsp72 is an intracellular target of the α,β-unsaturated sesquiterpene lactone, parthenolide, ACS Omega 2 (2017) 7267–7274.
[33] T. Varga, Z. Czimmerer, L. Nagy, PPARs are a unique set of fatty acid regulated transcription factors controlling both lipid metabolism and inflammation, Biochim. Biophys. Acta 1812 (2011) 1007–1022.
[34] S. Sauer, Ligands for the nuclear peroxisome proliferator-activated receptor gamma, Trends Pharmacol. Sci. 36 (2015) 688–704.
[35] I. Cuaranta-Monroy, M. Kiss, Z. Simandi, L. Nagy, Genomewide effects of peroxisome proliferator-activated receptor gamma in macrophages and dendritic cells -

revealing complexity through systems biology, Eur. J. Clin. Investig. 45 (2015) 964–975.
[36] A.M. Ferreira, et al., Macrophage activation induces formation of the anti- inflammatory lipid cholesteryl-nitrolinoleate, Biochem. J. 417 (2009) 223–234.
[37] G.S. Hotamisligil, D.A. Bernlohr, Metabolic functions of FABPs–mechanisms and therapeutic implications, Nat. Rev. Endocrinol. 11 (2015) 592–605.
[38] P.R.S. Baker, et al., Fatty acid transduction of nitric oxide signaling: multiple nitrated unsaturated fatty acid derivatives exist in human blood and urine and serve as endogenous peroxisome proliferator-activated receptor ligands, J. Biol. Chem. 280 (2005) 42464–42475.
[39] M. Fazzari, et al., Nitro-fatty acid pharmacokinetics in the adipose tissue compartment, J. Lipid Res. 58 (2017) 375–385.
[40] K.T. Hsu, J. Storch, Fatty acid transfer from liver and intestinal fatty acid-binding proteins to membranes occurs by different mechanisms, J. Biol. Chem. 271 (1996) 13317–13323.
[41] W. Chanput, J.J. Mes, H.J. Wichers, THP-1 cell line: an in vitro cell model for immune modulation approach, Int. Immunopharmacol. 23 (2014) 37–45.
[42] M. Furuhashi, et al., Treatment of diabetes and atherosclerosis by inhibiting fatty-acid-binding protein aP2, Nature 447 (2007) 959–965.
[43] A.V. Hertzel, et al., Identification and characterization of a small molecule inhibitor of fatty acid binding proteins, J. Med. Chem. 52 (2009) 6024–6031.
[44] H. Xu, et al., Uncoupling lipid metabolism from inflammation through fatty acid binding protein-dependent expression of UCP2, Mol. Cell. Biol. 35 (2015) 1055–1065.
[45] K.J. Livak, T.D. Schmittgen, Analysis of relative gene expression data using real-time quantitative PCR and the 2-ΔΔCT method, Methods 25 (2001) 402–408.
[46] J. Schindelin, et al., Fiji: an open-source platform for biological-image analysis, Nat. Methods 9 (2012) 676–682.
[47] L. Maria Curto, J. Javier Caramelo, G. Raquel Franchini, J. Maria Delfino, Delta 98 Delta, a minimalist model of antiparallel beta-sheet proteins based on intestinal fatty acid binding protein, Protein Sci. 18 (2009) 735–746.
[48] A.W. Norris, E. Li, Fluorometric titration of the CRABPs, in: C.P.F. Redfern (Ed.), Retinoid Protocols. Methods in Molecular Biology, vol. 89, Humana Press, 1998, pp. 123–139.
[49] Z.H. Xu, D.A. Bernlohr, L.J. Banaszak, The adipocyte lipid-binding protein at 1.6-a resolution - crystal-structures of the apoprotein and with bound saturated and unsaturated fatty-acids, J. Biol. Chem. 268 (1993) 7874–7884.
[50] D.A. Case, D.S. Cerrutti, T.A. Cheatham III, T.A. Darden, R.E. Duke, T.J. Giese, H. Gohlke, A.W. Goetz, D. Greene, N. Homeyer, S. Izadi, A. Kovalenko, T.S. Lee, S. LeGrand, P. Li, C. Lin, J. Liu, T. Luchko, R. Luo, D. Mermelstein, K.M. Merz, G. Monard, H. Nguyen, I. Omelyan, A. Onufriev, J. Wang, R.M. Wolf, X. Wu, L. Xiao, D.M. York, P. Kollman, AMBER16, University of California, San Francisco, 2017.
[51] F. Jensen, Introduction to Computational Chemistry, Wiley, 2017.
[52] Jacopo Tomasi, Benedetta Mennucci, R. Cammi, Quantum Mechanical Continuum Solvation Models, (2005), https://doi.org/10.1021/CR9904009.
[53] M.J. Frisch, G.W. Trucks, H.B. Schlegel, G.E. Scuseria, M.A. Robb, J.R. Cheeseman, G. Scalmani, V. Barone, B. Mennucci, G.A. Petersson, H. Nakatsuji, M. Caricato, X. Li, H.P. Hratchian, A.F. Izmaylov, J. Bloino, G. Zheng, J.L. Sonnenberg, M. Hada, M. Ehara, K. Toyota, R. Fukuda, C.J.F.D. Hasegaw, Gaussian 09 Revision D.01, Gaussian Inc., Wallingford, CT, USA, 2013.
[54] Peter A. Kollman, et al., Calculating Structures and Free Energies of Complex Molecules: Combining Molecular Mechanics and Continuum Models, (2000), https://doi.org/10.1021/AR000033J.
[55] B.R. Miller, et al., *MMPBSA.py* : an efficient program for end-state free energy calculations, J. Chem. Theory Comput. 8 (2012) 3314–3321.
[56] M.G. Wootan, N.M. Bass, D. a Bernlohr, J. Storch, Fatty acid binding sites of rodent adipocyte and heart fatty acid binding proteins: characterization using fluorescent fatty acids, Biochemistry 29 (1990) 9305–9311.
[57] G.V. Richieri, R.T. Ogata, A.M. Kleinfeld, Equilibrium constants for the binding of fatty acids with fatty acid-binding proteins from adipocyte, intestine, heart, and liver measured with the fluorescent probe ADIFAB, J. Biol. Chem. 269 (1994) 23918–23930.
[58] M.R. Rich, J.S. Evans, Molecular dynamics simulations of adipocyte lipid-binding protein: effect of electrostatics and acyl chain unsaturation, Biochemistry 35 (1996) 1506–1515.
[59] R.E. Gillilan, S.D. Ayers, N. Noy, Structural basis for activation of fatty acid-binding protein 4, J. Mol. Biol. 372 (2007) 1246–1260.
[60] Y. Li, X. Li, Z. Dong, Concerted dynamic motions of an FABP4 model and its ligands revealed by microsecond molecular dynamics simulations, Biochemistry 53 (2014) 6409–6417.
[61] N. Tan, et al., Selective cooperation between fatty acid binding proteins and peroxisome proliferator-activated receptors in regulating transcription selective cooperation between fatty acid binding proteins and peroxisome proliferator-activated receptors in regulating T, Mol. Cell. Biol. 22 (2002) 5114–5127.
[62] S.D. Ayers, K.L. Nedrow, R.E. Gillilan, N. Noy, Continuous nucleocytoplasmic shuttling underlies transcriptional activation of PPARgamma by FABP4, Biochemistry 46 (2007) 6744–6752.
[63] A. Adida, F. Spener, Adipocyte-type fatty acid-binding protein as inter-compartmental shuttle for peroxisome proliferator activated receptor γ agonists in cultured cell, Biochim. Biophys. Acta Mol. Cell Biol. Lipids 1761 (2006) 172–181.
[64] O. Rom, N.K.H. Khoo, Y.E. Chen, L. Villacorta, Inflammatory signaling and metabolic regulation by nitro-fatty acids, Nitric Oxide 78 (2018) 140–145.
[65] F.J. Schopfer, N.K.H. Khoo, Nitro-fatty acid logistics: formation, biodistribution, signaling, and pharmacology, Trends Endocrinol. Metab. (2019), https://doi.org/10.1016/J.TEM.2019.04.009.
[66] A.L. Hansen, et al., Nitro-fatty acids are formed in response to virus infection and are potent inhibitors of STING palmitoylation and signaling, Proc. Natl. Acad. Sci. U.S.A. 115 (2018) E7768–E7775.
[67] S.A. Kliewer, et al., Fatty acids and eicosanoids regulate gene expression through direct interactions with peroxisome proliferator-activated receptors alpha and gamma, Proc. Natl. Acad. Sci. U.S.A. 94 (1997) 4318–4323.
[68] A. Kasonga, M.C. Kruger, M. Coetzee, Activation of PPARs modulates signalling pathways and expression of regulatory genes in osteoclasts derived from human CD14+ monocytes, Int. J. Mol. Sci. 20 (2019).
[69] M. Fazzari, et al., Electrophilic fatty acid nitroalkenes are systemically transported and distributed upon esterification to complex lipids, J. Lipid Res. 60 (2019) 388–399.
[70] L. Turell, et al., The chemical basis of thiol addition to nitro-conjugated linoleic acid, a protective cell-signaling lipid, J. Biol. Chem. 292 (2017) 1145–1159.
[71] T. Olszowski, et al., Cadmium Alters the Concentration of Fatty Acids in THP-1 Macrophages, Biol Trace Elem Res 182 (2018) 29–36.
[72] S. Wallner, et al., Monocyte to macrophage differentiation goes along with modulation of the plasmalogen pattern through transcriptional regulation, PLoS One 9 (2014) e94102.
[73] H. Lu, et al., Novel gene regulatory networks identified in response to nitro-conjugated linoleic acid in human endothelial cells, Physiol. Genom. 51 (2019) 224–233.
[74] S. Li, et al., Transcriptomic sequencing reveals diverse adaptive gene expression responses of human vascular smooth muscle cells to nitro-conjugated linoleic acid, Physiol. Genom. 50 (2018) 287–295.
[75] M. Boß, M. Kemmerer, B. Brüne, D. Namgaladze, FABP4 inhibition suppresses PPARγ activity and VLDL-induced foam cell formation in IL-4-polarized human macrophages, Atherosclerosis 240 (2015) 424–430.
[76] I.M. Chrisman, et al., Defining a conformational ensemble that directs activation of PPARγ, Nat. Commun. 9 (2018) 1794.
[77] D.J.P. Bates, P.K. Smitherman, A.J. Townsend, S.B. King, C.S. Morrow, Nitroalkene fatty acids mediate activation of Nrf2/ARE-dependent and PPARγ-dependent transcription by distinct signaling pathways and with significantly different potencies, Biochemistry 50 (2011) 7765–7773.
[78] L. Turell, M. Steglich, B. Alvarez, The chemical foundations of nitroalkene fatty acid signaling through addition reactions with thiols, Nitric Oxide 78 (2018) 161–169.
[79] C.-S.C. Woodcock, et al., Nitro-fatty acid inhibition of triple-negative breast cancer cell viability, migration, invasion, and tumor growth, J. Biol. Chem. 293 (2018) 1120–1137.
[80] J.I. Odegaard, et al., Macrophage-specific PPARgamma controls alternative activation and improves insulin resistance, Nature 447 (2007) 1116–1120.
[81] A. Szanto, et al., STAT6 transcription factor is a facilitator of the nuclear receptor PPARγ-regulated gene expression in macrophages and dendritic cells, Immunity 33 (2010) 699.
[82] A.J. Covarrubias, et al., Akt-mTORC1 signaling regulates Acly to integrate metabolic input to control of macrophage activation, Elife 5 (2016).
[83] Z.S. Nagy, Z. Czimmerer, A. Szanto, L. Nagy, Pro-inflammatory cytokines negatively regulate PPARγ mediated gene expression in both human and murine macrophages via multiple mechanisms, Immunobiology 218 (2013) 1336–1344.